A hunt for *OM45* synthetic petite interactions in *Saccharomyces cerevisiae* reveals a role for Miro GTPase Gem1 in cristae structure maintenance

Antonina Shvetsova[a], Ali J. Masud [a], Laura Schneider[a], Ulrich Bergmann[a], Geoffray Monteuuis[a§], Ilkka J. Miinalainen[a], J. Kalervo Hiltunen[a], Alexander J. Kastaniotis[a#]

[a]Faculty of Biochemistry and Molecular Medicine and Biocenter Oulu, University of Oulu, Finland[a]

Running Head: Om45 and yeast IMM integrity

Keywords: *OM45*, *GEM1* Miro GTPase, *UGO1,* cristae organization, mtDNA inheritance.

[#]Address correspondence to alexander.kastaniotis@oulu.fi

[§]Present address: Geoffray Monteuuis, PhD, University of Helsinki, Department of Biochemistry and Developmental Biology, PO Box 63 (Haartmaninkatu 8), 00014 Helsinki, Finland

The data that support the findings of this study are available from the corresponding author upon reasonable request.

This work was funded by Biocenter Oulu, Academy of Finland and the Sigrid Jusélius Foundation.

No animals or humans were subjects of these studies.

The authors declare no conflicts of interest.

SUMMARY

Om45 is a major protein of the yeast outer mitochondrial membrane under respiratory conditions. However, the cellular role of the protein has remained obscure. Previously, deletion mutant phenotypes have not been found, and clear amino acid sequence similarities that would allow inferring its functional role are not available. In this work, we describe synthetic petite mutants of *UGO1* and *GEM1* that depend on the presence of *OM45* for respiratory growth, as well as the identification of several multicopy suppressors of the synthetic petite phenotypes. In the analysis of our mutants, we demonstrate that Om45 and Gem1 have a collaborative role in the maintenance of mitochondrial morphology, cristae structure and mitochondrial DNA maintenance. A group of multicopy suppressors rescuing the synthetic lethal phenotypes of the mutants on non-fermentable carbon source additionally supports this result. Our results imply that the synthetic petite phenotypes we observed are due to the disturbance of the inner mitochondrial membrane and point to this mitochondrial sub-compartment as the main target of action of Om45, Ugo1 and the yeast Miro GTPase Gem1.

Keywords: OM45, *GEM1*, Miro GTPase, *UGO1,* cardiolipin, mitochondria, outer and inner mitochondrial membranes, mtDNA inheritance

INTRODUCTION

The outer mitochondrial membrane (OMM) is the cytosol-exposed subcompartment that serves as an interface between the organelle and the rest of the cell. It is the first physical barrier of the organelle, restricting access to the mitochondrial intermembrane space to solutes smaller than 5 kDa (Mannella, 1992; Vander Heiden *et al.*, 2000). Om45p in the yeast *Saccharomyces cerevisiae* has been previously recognized as a major OMM protein in respiring yeast cells (Yaffe *et al.*, 1989; Ohlmeier *et al.*, 2004). The change in the expression of Om45p upon shift from growth on the fermentable carbon source glucose to glycerol is more than a magnitude higher than the general increase of mitochondrial proteins following the diauxic shift (Ohlmeier *et al.*, 2004). Hence, Om45p is expected to have a role for mitochondrial functions. Surprisingly, an *om45* knockout yeast strain showed no detectable phenotype under numerous conditions investigated (Yaffe *et al.*, 1989). A C-terminally tagged GFP Om45p is commonly used as a mitochondrial marker in studies of mitochondrial morphology and mitophagy (Sesaki *et al.*, 2001; Kanki *et al.*, 2009).

Om45p is a membrane-anchored protein consisting of a short hydrophobic N-terminal transmembrane sequence of 22 amino acids and the remaining bulk of the protein constituting a water-soluble domain. For a long time, the latter had been described as facing the cytoplasm (Riezman *et al.*, 1983; Yaffe *et al.*, 1989; Waizenegger *et al.*, 2003; Burri *et al.*, 2006). Lauffer *et al*. first reported evidence for an intermembrane space orientation of the Om45p C-terminus along with data indicating association of Om45 with yeast mitochondrial OMM proteins Por1p and Om14p. This high molecular weight complex interacts physically with the components of the IMM: transporters, adenine nucleotides carrier, the prohibitin complex, respiratory chain

complexes III and IV, as well as ATP synthase (Lauffer *et al.*, 2012). Evidence presented by both Song *et al.* and Wenz *et al.* (Song *et al.*, 2014; Wenz *et al.*, 2014) indicate that Om45p insertion into the OMM is also dependent on protein factors and not only on the lipid composition of the OMM as had been previously suggested.

Here, we describe the results of a screen for mutations interacting negatively with a deletion allele of *OM45* revealing a role for its gene product in preserving inner mitochondrial membrane morphology. Using a colony-color-based synthetic petite screening approach in *S. cerevisiae*, we isolated three mutants which display a respiratory growth defect in the absence of Om45p. We tracked the source of the mutant phenotypes to point mutations to two distinct genes encoding the evolutionarily conserved OMM proteins, Ugo1 and Gem1. Deletions of the genes encoding these factors have been previously reported to lead to disturbed mitochondrial morphology (Sesaki *et al.*, 2001; Frederick *et al.*, 2004; Coonrod *et al.*, 2007; Abrams *et al.*, 2015). Our data presented here provide evidence for a joint function of Om45p and Gem1 in mitochondrial cristae structure maintenance and dynamics, and a requirement for *OM45* for mitochondrial DNA (mtDNA) maintenance upon inactivation of its genetically interacting partner *GEM1*.

RESULTS

Synthetic petite screen

It has been previously reported that Om45p is not essential for the yeast growth or mitochondrial functions (Yaffe *et al.*, 1989). Our W1536 8B *om45* deletion strain, a derivative of W303, grew equally well as the corresponding wild-type strain under the growth conditions investigated (Supplementary Fig.1). We hypothesized that the absence of any growth phenotype for the major protein of the OMM may be due to the presence of (a) protein(s) with redundant functions. This possibility was addressed in a screen for synthetic petite mutants (SPM) (Kursu *et al.*, 2013). (Fig. 1A). The screen was designed to identify mutations that in absence of *OM45* would lead to a synthetic growth defect specifically on non-fermentable media containing glycerol, but not on fermentable media containing glucose. Following this idea, we screened over 50000 colonies and obtained three stable synthetic petite mutants in a Δ*om45* strain background that were dependent on an *OM45* plasmid for growth on SCG after chemical mutagenesis. These mutants readily lost the *OM45* plasmid on SCD, upon which they became respiratory deficient, and were viable on fermentable carbon sources in absence of *OM45* (Fig. 1B and C). Upon loss of the *OM45*-containing plasmid, it was not possible to complement the synthetic petite mutants with any plasmid encoding the intact copies of *OM45*. Hence, all the complementation experiments and cloning of the mutations by library complementation were done via plasmid shuffle. The obtained synthetic petite mutants were recessive, as diploids of the Δ*om45* parentals with the SPMs are respiratory competent in absence of the *OM45* plasmid.

Synthetic mutations in the *GEM1* and *UGO1* genes

The gene alleles with acquired point mutations in the three synthetic petite mutant yeast lines were identified by cloning based on genomic DNA library complementation. For this purpose, two yeast multicopy genomic DNA libraries: HeAl (Kastaniotis *et al.*, 2004) and Lacroute (Bonneaud *et al.*, 1991; Harington *et al.*, 1993) were used for transformation of the synthetic petite mutants carrying the YEp112*OM45* plasmid. The latter construct carries a *TRP1* marker gene that can be selected against on 5' fluoroanthranilic acid (5'FAA)-containing media. From about 50000 independent transformants able to grow on selective media supplemented with glycerol upon loss of the YEp112*OM45* plasmid, several independent clones containing *OM45* were isolated during our library complementation screen, confirming the good quality of the library and the validity of the cloning strategy. We tracked the cause of the mutant phenotype of the synthetic petite strains to point mutations in two distinct genes encoding OMM proteins Ugo1, a participant in the mitochondrial fusion machinery (Sesaki *et al.*, 2001), and Gem1p, the mitochondrial Rho (Miro) GTPase (Frederick *et al.*, 2004). Single copy plasmids carrying wild-type alleles of these plasmids complemented as well as the original multicopy (2μ) library plasmids. Sequencing of the mutant alleles revealed a transition mutation in *ugo1*(c.566C>T), translating to p.P189L in the mutant ugo1 protein. This mutation is located in a segment of the Ugo1 amino acid sequence that is exposed to the inter membrane space (IMS) (Hoppins *et al.*, 2009). We mapped the *gem1-1* (c.308G>A/ p.R103K) mutation to the first GTPase domain of Gem1 and *gem1-2* (c.971G>A/ p.S324N) to the region between the two EF hands domains of the protein (Frederick *et al.*, 2004) (Fig. 1 D and E). The *OM45* genetic interactions with both *GEM1* and *UGO1* found in our screen are consistent with high throughput yeast synthetic lethality data reported before (Hoppins *et al.*,

2011). The Gem1 and Ugo1 proteins have previously been shown to play a role in yeast mitochondrial morphology maintenance (Frederick *et al.*, 2004; Sesaki *et al.*, 2004).

Mitochondrial morphology defects in synthetic petite mutants devoid of *OM45* plasmid

In addition to the growth defects, SPM demonstrated changes in mitochondrial structure. We examined mitochondrial morphology in SPMs in the presence and absence of an *OM45* plasmid (Fig. 2). Mitochondria of the *ugo1* (p.P189L) SPM strain grown on glucose media displayed many fragmented, collapsed mitochondria in the close proximity to each other, nonetheless apparently unable to fuse and form the long tubular structures that can be found in the WT control. Presence of the plasmid copy of *OM45* slightly ameliorated the phenotype and some tubular-like mitochondria were present. SPMs of *gem1*(p.R103K) and *gem1*(p.S324) (not shown) also contained many fragmented and collapsed mitochondria. Some tubular mitochondrial structures were present in these mutant cells, although the diameter of such tubules was irregular, they appeared collapsed and reminiscent of a "beads on a string" arrangement. Presence of the plasmid borne of *OM45* improved this phenotype, resulting in mitochondria with more tubular structure and more regular in diameter (Fig. 2, Fig.3).

Electron microscopy analysis of the SPMs with and without the plasmid copy of *OM45* revealed defects in the folding of the inner mitochondrial membrane (IMM) (Fig. 4). The double membranes of mitochondria were clearly observed, but the IMM was completely devoid of regular cristae organization and was found either adjacent to the OMM or forming a stretch along the mitochondria approaching the OMM at both ends or displaying small circles. In contrast, the cristae organization of W303 strain background cells carrying the Δ*gem1* mutation alone has been reported to be unaffected (Frederick *et al.*, 2004) and the IMM of W1536 8B Δ*om45* strain is

141 indistinguishable from wild type under regular growth conditions. These results indicated a
142 synthetic negative effect of *om45* and *gem1* mutations on IMM structure. The presence of a
143 multicopy *OM45*-carrying plasmid visibly relieved the severity of the phenotype, largely restoring
144 classical cristae organization of most mitochondria.

145 **Reconstruction of the mutants**

146 In order to better characterize the SPMs, we performed tetrad analysis of Δ*om45*/ Δ*om45*-SMP
147 diploids. The dissection pattern of the mutants during the tetrad analysis (Supplementary Fig. 2)
148 did not follow Mendelian segregation. If only one mutation was involved we would expect a clear
149 2:2 (viable:non-viable) segregation pattern on glycerol. In case two mutations were required to get
150 the respiratory deficient phenotype in the Δ*om45* background, we would expect: 2:2 for the
151 parental ditype, 4:0 for the non-parental ditype, and 3:1 for the tetratype. There is no scenario
152 following Mendelian genetics that would ever result in a 0:4 (respiratory competent:respiratory
153 deficient) ratio, which we frequently encountered in the tetrad dissection analysis of the *gem1*
154 SPMs. Tetrad analysis of the *ugo1* SPM yielded many 4:0 (respiratory competent:respiratory
155 deficient) and a few 3:1 tetrads, not consistent with a simple relationship between the Δ*om45*
156 genetic background and the *ugo1* SPM.

157 In our interpretation, the erratic inheritance pattern of the *gem1* SPMs was caused by disturbed
158 mitochondrial DNA inheritance. Because this feature of our mutants interfered with our attempts
159 to breed out possible background mutations, and to investigate or completely rule out the
160 possibility of a complex combination of several nuclear mutations as the root of the non-
161 Mendelian segregation pattern, we reconstructed the mutant genotype in cells that had not been
162 exposed to EMS mutagenesis.

The W1536 8B Δ*gem1*Δ*om45* double deletion strain was created by introducing the *HPHMX* KO cassette (conferring hygromycin resistance) into the *GEM1* locus the W1536 8B *Δom45* strain, thereby removing *GEM1*. Neither of the single deletion strains (Δ*gem1* or Δ*om45*) are respiratory deficient (Yaffe *et al.*, 1989; Frederick *et al.*, 2004). The obtained Δ*gem1*Δ*om45* double deletion strain, in contrast to the *gem1* point mutation SPMs, was initially not respiratory deficient but a very slow grower on glycerol containing media. The Δ*om45gem1*(R103K) and Δ*om45gem1*(S324N) point mutants were reconstructed by introduction of the plasmid-borne *gem1* (R103K) and *gem1*(S324N) alleles into the W1536 8B Δ*gem1*Δ*om45* double deletion strain. The behavior of these three reconstructed strains under different growth conditions was tested (Fig. 5A). A plasmid harboring wild type *GEM1* (YCp33*GEM1*) completely rescued the growth of the W1536 8B Δ*gem1*Δ*om45* strain, whereas YCp33*gem1* (R103K) and YCp33*gem1* (S324N) rescued the growth only partially, (Fig. 5A).

Since the *ugo1* null mutant is respiratory deficient as a result of mtDNA loss subsequent to the loss of *UGO1* (Sesaki *et al.*, 2001), reconstruction of the strain was achieved *via* plasmid shuffle. The *UGO1* gene was knocked out in the presence of a plasmid carrying a wild-type *UGO1* allele and the *ugo1* (P189L) allele was then introduced with a second plasmid, selecting against the initial construct carrying the wild-type copy. On the non-fermentable media SCG the growth of the Δ*om45, Δugo1/ugo1*(P189L) reconstructed synthetic petite mutant was strongly reduced. The pTSV30*OM45* construct as well as the plasmid harboring an intact copy of *UGO1* rescued the respiratory growth of the reconstructed mutant (Supplementary Fig. 3).

The reconstruction of the mutants confirmed the negative synthetic interaction of the *om45* deletion with the *ugo1* and *gem1* mutations. As Ugo1p is poorly defined and the synthetic petite

interaction was more robust for the reconstructed Δ*om45*/*gem1* mutant strains, we decided to focus on the *gem1*/*om45* interaction for our further analyses.

Electron microscopy analysis of the Δ*om45*Δ*gem1* double mutant revealed mitochondrial membrane defects (Fig. 5B) similar to the phenotype we observed in the SPMs (Fig. 4 B, D). The cristae structure of the IMM was severely disturbed or completely absent. However, when these cells were transformed with a plasmid carrying *OM45*, cristae were restored (Fig. 5 C) and the mitochondria in the transformed strain were much closer to the appearance of WT organelles (Fig 5 D), again mimicking the behavior of the SPM strains (Fig. 4 A, C). Overall, the reconstructed mutants as well as the Δ*om45*Δ*gem1* double deletion mutant very closely resembled the original SPMs in their phenotypes.

The Δ*om45*Δ*gem1* strain generates petites at high frequency when grown on fermentable media

While W1536 8B Δ*gem1*Δ*om45* cells can be maintained indefinitely growing, albeit slowly, on glycerol media, a large fraction of the W1536 8B Δ*gem1*Δ*om45* cells similarly to original SPM became completely respiratory deficient after just a brief growth phase on glucose media, and could not be rescued anymore with plasmids carrying *OM45* or the *GEM1*. Similarly, we observed that the original synthetic petite mutants, once they had lost the initial *OM45* plasmid upon maintenance on glucose containing medium, could not be rescued again by the re-transformation with a 2μ *OM45* plasmid.

We compared the frequency of generation of petites between W1536 8B Δ*om45,* W1536 8B Δ*gem1* and W1536 8B Δ*om45*Δ*gem1* strains, starting from cells growing on glycerol. After transfer to liquid YPD with a fermentable carbon source and overnight growth, cells were plated

on a YPD plate, grown 4-5 days until proper colonies were formed and subsequently replica plated onto non-fermentable SCG media (Fig. 5 E). W1536 8B Δ*om45* formed only very few respiratory deficient petite colonies. The W1536 8B Δ*gem1* mutant, which had previously been reported as losing mtDNA at slightly elevated rate (Frederick *et al.*, 2004), generated up to 15% of respiratory deficient colonies. The Δ*gem1*Δ*om45* petite generation rate under the same conditions approached 85%. Therefore, percentage of generation of respiratory deficient progeny was strongly increased in the Δ*om45*Δ*gem1* double mutant compared to the individual deletion strains (Fig. 5 F).

We hypothesized that this high frequency generation of petites is caused by mtDNA loss, which would be consistent with our inability to complement the SMPs with plasmids carrying wild type copies of *OM45* (or *GEM1/UGO1*) once the *OM45* plasmid was lost.

Synthetic petite mutants and mtDNA maintenance

Respiratory competence of the SPMs upon loss of the OM45 plasmid could not be restored upon re-transformation. To investigate DNA copy number in wild type, Δ*om45* and Δ*gem1* mutants as well as the Δ*om45,* Δ*gem1* double mutant, we performed droplet digital PCR (ddPCR) probing for the mtDNA encoded *COX3* (cytochrome c oxidase subunit 3) gene and nuclear encoded *ACT1* as reference. We found that the Δ*om45* mutant harbored mtDNA to wild type levels, while the Δ*gem1* strain exhibited a slight reduction of mtDNA when grown on non-fermentable glycerol. Intriguingly, the Δ*om45,* Δ*gem1* double deletion mutant appeared to even exhibit a slight increase *COX3* copy number when grown on glycerol (Fig. 5G). This is in stark contrast to the situation after the Δ*om45,* Δ*gem1* strain was subjected to overnight growth on fermentable YPD (Fig. 5G) and mtDNA content was massively reduced (Fig. 5G). The irreversible respiratory defect can be caused by either distortion of mitochondrial genome integrity (rho^{-}) or by its complete loss (rho^{0}).

A DAPI stain of SPM mutant cells showed a severe reduction of fluorescent spots co-localizing with mitochondrial matrix targeted GFP protein in absence of an OM45-carrying plasmid. This phenotype is more consistent with a reduction of mtDNA copy number in the SPMs than with deletions within the mitochondrial DNA as cause for secondary respiratoy deficiency (Supplementary Fig. 4).

Suppression of SPM phenotypes.

In addition to *UGO1*, *GEM1* and *OM45,* several other genes from the two rescuing library plasmids were identified and found to be suppressors of the mutations in *gem1* and *ugo1* genes (Supplementary Table 1, Supplementary Fig. 5 and 6). Among these suppressors are genes encoding proteins of both the IMM (*TIM44, SHY1*, *RTT109, PET9*) and the OMM (*FZO1, MCP1* and *PET54*). The *MCP1, PET54* and *YPL109c* partially rescued the growth of all three mutants also from a single copy plasmid, but no mutation was detected in the genomic copies of the genes. Respiratory growth of Δ*om45 ugo1* (P189L) SPMs was restored by multicopy plasmids carrying *TIM44, SHY1, DNM1* and *FZO1*

Functionality of Om45p fusion constructs

Om45p-GFP constructs have been used for mitochondrial morphology as well as autophagy studies due to Om45p abundance in the OMM during respiration and a previously reported lack of a phenotype for the W1536 8B Δ*om45* strain (Sesaki *et al.*, 2001; Kanki *et al.*, 2009). The reconstructed synthetic petite mutant W1536 8B Δ*om45*Δ*gem1* strain serves as a unique working tool for testing the functionality of Om45p and its fusion constructs.

First, we performed the complementation analysis of our mutants with an Om45p-GFP construct. The GFP-tagged *OM45* single and multicopy plasmids (YCp33*OM45-GFP* and YEp195*OM45-GFP)* rescued the respiratory growth of the W1536 8B Δ*om45*Δ*gem1* mutants much weaker than the plasmids carrying native *OM45* (Fig. 6 A). This effect could be observed already in the sole W1536 8B Δ*om45* mutant, although much less pronounced (Fig. 6 B). Western blot analysis indicated that the levels of expression of Om45p and Om45-GFP were similar (Fig. 6 C).

In the case of the Δ*om45, ugo1*(P189L) SPM, the OM45-GFP is not rescuing the respiratory deficient phenotype of the mutant strain at all (Fig. 6 D).

Phospholipid analysis

The results of the synthetic lethal screen implied that Gem1p and Om45p are likely to have some redundancy in their physiological roles. It has been suggested that Gem1p may regulate ER-mitochondria tethering, although the *gem1* deletion alone is not sufficient to impair the phospholipid (PL) trafficking between ER and mitochondria (Nguyen *et al.*, 2012). We decided to investigate whether *GEM1* loss in combination with the *om45* deletion leads to impaired ER-mitochondria interaction. Phosphatidyl choline (PC) synthesis from phosphatidylserine (PS) in yeast requires proper tethering of ER with OMM (Daum *et al.*, 1997; Carman *et al.*, 1999; Stone *et al.*, 2000; Kornmann *et al.*, 2011; Nguyen *et al.*, 2012; Horvath *et al.*, 2013). In order to develop an ER-mitochondria interaction assay we sought to take advantage of this dependence of the phospholipid biosynthesis process on a tight association of the two organelles.

In addition to the mitochondrial PS decarboxylation, there is a minor vacuolar/Golgi pathway in yeast involving Psd2p, which does not depend on mitochondria-ER interaction. In order to study exclusively the contribution of mitochondrial PS-synthesis, all strains were generated in a Δ*psd2*

background (Trotter *et al.*, 1993; Trotter *et al.*, 1995; Voelker, 1997). If Om45p and Gem1p had a redundant function in mediating ER-mitochondria interaction, the Δ*psd2*Δ*gem1*Δ*om45* triple knockout strain would be predicted to show an accumulation of PS and possibly depletion of phosphatidylethanolamine (PE) or PC due to impaired trafficking between ER and mitochondria. A suitable control is the isogenic W1536 8B Δ*psd1*Δ*psd2* strain, where deletion of both PS decarboxylase enzymes severely compromises phospholipid metabolism, leading to accumulation of unprocessed PS. As additional controls, phospholipid profiles of W1536 8B Δ*gem1* or W1536 8B Δ*om45* deletion strains also lacking *psd2* were investigated to assess the effect of the individual deletions of these OMM proteins on phospholipid turnover.

UPLC-Q-Tof-MS was used to analyze the lipidomes of whole cells and of highly purified mitochondria from five different deletion strains grown on glycerol containing media: W1536 8B Δ*om45*Δ*psd2*; W1536 8B Δ*gem1*Δ*psd2*; W1536 8B Δ*gem1*Δ*om45*Δ*psd2*; W1536 8B Δ*psd2* and Δ*psd1*Δ*psd2* (Supplementary Fig. 6). The W1536 8B Δ*psd1*Δ*psd2* control strain lacking both PS decarboxylases is an auxotroph for ethanolamine required to produce the essential PE and PC phospholipids via the Kennedy pathway (McMaster, 2018). Hence, growth media of all strains were supplemented with 2 mM ethanolamine. Growth of strains on glycerol is cumbersome especially for the very slow growing Δ*gem1*Δ*om45*Δ*psd2* variant, but as we wanted to avoid lesions secondary to the original mutations, it was necessary to produce cell material under conditions that prevented mtDNA loss.

Our mass spectrometric PL analysis was consistent with the results of Vance *et al*., who demonstrated that PC is the most abundant PL in eukaryotic cells. PE and PI are also present in ample amounts, while PS, a precursor for PE and PC is quantitatively a minor phospholipid

293 (Vance *et al.*, 2005) (Supplementary Fig. 6) The data are presented in the % ratios, with the total
294 sample phospholipids set as100% as well as PS/PE ratio.

295 As expected, the PS/PE ratio showed a clear increase in W1536 8B Δ*psd1*Δ*psd2* strain, where
296 deletion of both PS decarboxylase enzymes severely compromised phospholipid metabolism and
297 caused PS accumulation. W1536 8B Δ*gem1*Δ*om45*Δ*psd2* did not show any increase in PS, and the
298 PS/PE ratio in this strain was similar to the control W1536 8B Δ*om45*Δ*psd2*, W1536 8B
299 Δ*gem1*Δ*psd2* and W1536 8B Δ*psd2* strains both in whole cell lipids extracts and in the highly pure
300 mitochondria. Thus, neither the *om45* deletion alone nor in combination with the *gem1* deletion
301 appear to affect the PS to PE conversion in yeast cells.

302 DISCUSSION

303 The cellular role of Om45, one of the major proteins of the yeast OMM, has remained obscure for
304 several decades. The protein is fixed to the OMM via an N-terminal α-helical membrane anchor,
305 and for a long time, it was believed that the major solvent exposed C-terminal domain of Om45
306 was facing the cytosol. Hence the place of action of Om45 was suspected to be on the
307 mitochondrial outer surface. Only in 2012 Lauffer *et al.* first reported evidence for the IMS
308 orientation of Om45 (Lauffer *et al.*, 2012). Data obtained by us in this present study are consistent
309 with the configuration proposed in the latter work.

310 The discovery of yeast Miro GTPase in the early 2000s initially caused a stir in the mitochondrial
311 community (Frederick *et al.*, 2004). Reports of a role of Gem1 as a partner of the ERMES
312 complex, regulating mitochondria-ER interactions and phospholipid exchange (Kornmann *et al.*,
313 2011) could not be unequivocally confirmed (Nguyen *et al.*, 2012). Here, we present evidence for
314 a collaborative role of Om45 and Gem1 in mitochondrial inner membrane organization. We were

315 unable to find any support for a function of these proteins, either alone or in combination, in
316 phospholipid trafficking. Our results imply that the action of Gem1 and Om45 is oriented towards
317 the IMM and required for cristae and mtDNA maintenance.

318 Our synthetic lethal screen based on the colony-color-sectoring-assay revealed two evolutionarily
319 conserved genes, *GEM1* and *UGO1*, as interacting genetically with *OM45*. The SPMs obtained in
320 our screen as well as the mutant reconstruction variants showed impaired IMM organization in the
321 absence of Om45 where they also become respiratory deficient due to progressive mtDNA loss.
322 The data speak in favor of at least partial redundancy of Om45 with Gem1 and Ugo1 in terms of
323 their physiological function. Unlike for Gem1 and Ugo1, which are conserved in higher
324 eukaryotes, no homolog of Om45 could be identified in mammals. Deletions of either *GEM1* or
325 *UGO1* have been shown to affect mitochondria morphology and mtDNA maintenance in yeast.
326 While Δ*gem1* strains experience only a mild increase of mtDNA loss (Frederick *et al.*, 2004), the
327 *ugo1* deletion results in a rho^0 phenotype (Sesaki *et al.*, 2001). Our Δ*om45*, Δ*gem1* double deletion
328 strain and *gem1* SPMs display a similar loss of mtDNA.

329 The Ugo1 protein has been reported to bring together OMM and IMM by acting as a scaffold
330 between Mgm1 and Fzo1 proteins in the IMM and the OMM, respectively (Sesaki *et al.*, 2004;
331 Coonrod *et al.*, 2007; Anton *et al.*, 2011). There have been speculations about a possible lipid
332 mixing role of Ugo1 required for mitochondrial fusion (Hoppins *et al.*, 2009). Cells lacking Ugo1
333 fail to form a tubular mitochondrial network, shifting the mitochondrial dynamics balance towards
334 fragmentation, which ultimately leads to complete loss of mtDNA (Sesaki *et al.*, 2001; Sesaki *et*
335 *al.*, 2004; Itoh *et al.*, 2013). Mutations in the Ugo1-like protein SLC25A46 in humans were
336 reported to cause an optic atrophy spectrum disorder. In contrast to the phenotype of *UGO1*
337 deletions in yeast, the knock down of *SLC25A46* was found to cause mitochondrial hyperfusion,

while overexpression of the mammalian *UGO1* homolog led to mitochondrial fragmentation (Abrams *et al.*, 2015). While we did not pursue any deeper analysis of the Δ*om45, ugo1* SPM, our ability to identify such an interaction in general supports our conclusions on the functions of Om45 and Gem1.

Gem1 is the yeast homolog of human Miro GTPase (Frederick *et al.*, 2004; Tang, 2015). In the absence of Gem1, yeast mitochondria exhibit a pronounced defect in mitochondrial cellular distribution and morphology, forming collapsed tubular and globular mitochondria with an irregular diameter (Frederick *et al.*, 2004). Unlike for its mammalian homolog, a role of Gem1 in interaction with the cytoskeleton has not been observed in yeast. Instead, deletion of *GEM1* has been reported to affect the size and the number of mitochondria-ER encounter structures (ERMES) in *S. cerevisiae.* The role of Gem1 in ERMES function has been controversial (Nguyen *et al.*, 2012). In our eyes, the synthetic defect in Δ*om45/gem(R103K),* Δ*om45/gem(S324N)* and Δ*om45 /ugo1(P189L)* can be only explained by (partially) redundant function(s) of the proteins acting in parallel. Inspired by experiments described previously for Δ*gem1* strains by the Shaw group (Nguyen *et al.*, 2012), we examined the phospholipid composition of the Δ*om45* and Δ*gem1* strains in order to determine if the redundant functions of Om45 and Gem1 may be obscuring an effect of the Δ*gem1* mutation on phospholipid levels and, by extension, on ERMES function. Like in the Nguyen *et al.* report, PS conversion to PE and further to PC in the yeast carrying single deletions of Δ*om45,* or Δ*gem1* as well as in the Δ*om45*Δ*gem1* double deletion was not distinguishable from the control. Hence, we found no evidence for a possible common role of the two proteins in mediating tethering of mitochondria to the ER.

Genetic interaction of *OM45* with *GEM1* was previously reported in a high throughput study describing components of the mitochondrial contact site (MICOS) complex (Hoppins *et al.*, 2011),

a scaffold-like structure required for mitochondrial IMM organization (Rabl *et al.*, 2009; Harner *et al.*, 2011; Alkhaja *et al.*, 2012; van der Laan *et al.*, 2012; Zerbes *et al.*, 2012; Pfanner *et al.*, 2014). Our SPMs are characterized by strong distortion of IMM folding, which may be a reason for progressive mtDNA loss. Our observation that the Δ*om45/*Δ*gem1* mutant appears to harbor increased amounts of mtDNA when the cells are maintained on glycerol as the sole carbon source is initially counterintuitive. A simple explanation, however, may be that under this condition (double deletion mutant cells forced to survive on glycerol) there is a selection for cells that maintain higher than normal amounts of mtDNA. A higher mtDNA copy number may help the cells to compensate for mitochondrial dysfunction caused by absence of the Om45 and Gem1 proteins. Maintenance of mtDNA in the glycerol-grown cells also indicates that loss of mtDNA is not likely to be the driving lesion in the SPMs but a consequence of the IMM defect of Δ*om45/* Δ*gem1* mutants.

It is intriguing that the combination of mutations in OMM proteins causes the strongest phenotype in the IMM folding. The reported IMS orientation of Om45p (Lauffer *et al.*, 2012; Song *et al.*, 2014; Wenz *et al.*, 2014), however, makes a role of the protein in the mediation of OMM and IMM contacts plausible.

In addition to the *GEM1* and *UGO1* isolates obtained by library complementation, we found several multicopy suppressors that can rescue the synthetic petite phenotypes. Among them are *FZO1, MCP1* encoding OMM proteins, as well as *TIM44, SHY1, PET9,* and *PET54* encoding IMM proteins. The function of Mcp1 is not well understood, but it appears to be involved in lipid homeostasis (Tan *et al.*, 2013). Physical interaction of Fzo1 with Ugo1 is required for mitochondrial fusion (Sesaki *et al.*, 2004; Coonrod *et al.*, 2007; Anton *et al.*, 2011). Shy1 and Pet54 play roles in respiratory complex IV component expression and assembly (Barrientos A, et

al. (2002) Shy1p is necessary for full expression of mitochondrial *COX1* in the yeast model of Leigh's syndrome. EMBO J 21(1-2):43-52, Costanzo MC, et al. (1989) The PET54 gene of Saccharomyces cerevisiae: characterization of a nuclear gene encoding a mitochondrial translational activator and subcellular localization of its product. Genetics 122(2):297-305). Pet9 (Aac2) is an ADP/ATP carrier of the IMM, affecting the level of ATP in the IMS and also found to be associated with MICOS and Om45-Om14-Por1 protein complexes (Lauffer *et al.*, 2012; Linden *et al.*, 2020). Tim44 is an essential component of the TIM23 complex (Blom *et al.*, 1993; Pfanner *et al.*, 1996; Popov−Čeleketić *et al.*, 2008), physically interacting with Ssc1 (Liu *et al.*, 2001; Wadhwa *et al.*, 2002; D'Silva *et al.*, 2004), which was found down-regulated in a proteomic study of the Δ*om45* strain. While we do not clearly understand the mechanisms of multicopy suppression by these factors as whole they point towards membrane fusion and protein import into the mitochondrial matrix as well as respiratory chain assembly functions. As the protein import machinery constitutes points of interaction between the two mitochondrial membranes, increased protein import due to higher respiratory chain assembly activity may be a possible mechanism for (partial) restoration of the IMM morphology. The increased mtDNA content we detected in the Δ*om45*Δ*gem1* SPM is consistent with this notion.

In spite of the fact that Om45 and Gem1 (as well as Ugo1) reside on the OMM, our results firmly indicate the IMM is most strongly affected by loss of function of these proteins action. Our investigation of the role of Om45 under growth conditions that have not been tested before as well as the genetic and physical interactions of Om45 that were identified during the course of this work revealed several cellular processes affected by Om45. In particular, mitochondrial morphology maintenance, IMM folding and mtDNA inheritance are affected by the absence of Om45 in a *gem1* (or *ugo1*) mutant strain background. Taken together, the mutant morphology,

407 growth phenotypes, multicopy suppressors and phospholipidome studies we present here point to
408 a possible role of Om45 and Gem1 in IMM homeostasis and mediation of interaction between the
409 two mitochondrial membranes. We find no direct evidence for a role of these proteins in
410 ER/mitochondrial phospholipid exchange processes.

411 An additional aspect of our work is that the phenotype of the synthetic mutant strains is strongly
412 dependent on the presence of Om45, which makes these synthetic petites a unique system for
413 testing the functionality of Om45 constructs. Our results indicate that C-terminal tagging of Om45
414 interferes with its functions. GFP-tagged Om45 did not complement the synthetic mutants and
415 displayed a growth defect in the Δ*gem1*Δ*om45* and Δ*om45* strain backgrounds. In light of our
416 observation of a role of Om45 in mitochondrial morphology maintenance, such constructs may not
417 be the best choice as a marker for mitochondrial morphology studies for which it has been used
418 previously (Sesaki *et al.*, 2001; Sesaki *et al.*, 2003).

419

420

421

422

423

424

425

426

427

428

EXPERIMENTAL PROCEDURES

Escherichia coli strains and growth media

The *E. coli* strain TOP10 was used for plasmid cloning and propagation (Invitrogen, Carlsbad, CA, USA). *E. coli* BL21 (DE3) (Studier *et al.*, 1986; Studier *et al.*, 1990) was used for protein production for antibody raising. *E. coli* was cultivated on LB media/agar plates (10 g tryptone, 5 g yeast extract, and 10 g NaCl in 1 L) or LB media/agar plates supplemented with ampicillin 100 µg/ml or chloramphenicol 100 µg/ml. Super optimal broth with catabolite repression (SOC) (2% tryptone, 0.5% yeast extract, 10 mM NaCl, 2.5 mM KCl, 20 mM glucose, 10 mM $MgCl_2$) was used during *E. coli* chemical transformation and electroporation.

Plasmids used in this study

For the plasmids used in the study, see Table 1. Plasmid construction was done using standard techniques (Ausubel *et al.*, 1989). All new constructs were sequence-verified.

Yeast strains and growth conditions

For yeast strains used in this work see Table 2. All the strains were derivatives of W1536 8B (Zhao *et al.*, 1998; Kastaniotis *et al.*, 2004). Yeast strains were grown in either rich YPD medium (1% yeast extract, 2% peptone and 2% D-glucose), YPG (3% glycerol), synthetic complete (SC) or synthetic complete drop-out media Kaiser mix (Formedium™, Hunstanton, Norfolk, United Kingdom or Sigma-Aldrich, St. Louis, MO, USA) SCD (2% D-glucose), SCG (3% glycerol) or SC media lacking one or more nutrients. Media were solidified with 2% Bacto agar [Biokar – (Sigma-Aldrich)]. Glycerol sectoring medium (GSM) was SCG medium supplemented with

0.05% glucose. The glucose supplementation is necessary for red color development of the W1536 8B strain on glycerol (Kastaniotis *et al.*, 2004).

Yeast transformation

Yeast one-step transformation was carried out as described earlier (Chen *et al.*, 1992) with minor modifications. Briefly, yeast cells from 300 µl of overnight culture were sedimented by a short spin in a table centrifuge (10 sec, 11000g). The supernatant was removed and the cells re-suspended in 100 µl of the transformation mix [0.17 M lithium acetate, 34% polyethylene glycol 3350 (PEG), 100 mM DTT, 0.3 µg/µl single-stranded salmon or herring sperm DNA (ssDNA), 1 µl plasmid DNA (0.1 - 2 µg)]. The cells were incubated in the transformation mix for 30 min at 42°C, plated on the appropriate selective medium and incubated at 30°C for 3-7 days.

Yeast high efficiency transformation was performed following the method of Gietz and Woods (Daniel Gietz *et al.*, 2002). Yeast cells were re-inoculated from an overnight culture to fresh YPD (or appropriate selective medium) in order to obtain 5 x 10^6 cells/ml and incubated for 3-5 h in a shaker while completing 2 doublings. Cells were harvested by centrifuging for 5 min x 3000 g, washed once with sterile distilled H_2O and once with 100 mM lithium acetate. To each 4x10^6 cells 360 µl of the transformation mix [240 µl PEG (50% w/v), 36 µl 1.0 M. lithium acetate 2 µl ssDNA (10 mg/ml), 0.1 - 10 µg plus H_2O to a volume of 34 µl] were added. Afterwards cells were incubated for 50 min at 42°C. Transformed cells were incubated in YPD liquid medium for 2-4 h and plated onto the appropriate selective medium.

PCR-mediated gene replacement

All yeast knock-out strains were created by PCR-targeting with short flanking homology (PCR-mediated gene replacement). The homologous ends of the transferring DNA were introduced by primers with a short region (25 bases) homologous to the knockout cassette (KANMX or HPHMX) and a region (40-45 bases) homologous to the gene to be replaced (5'or 3' to the stop and start codons of the ORF of the gene) (Goldstein *et al.*, 1999; Knop *et al.*, 1999). The resulting PCR product therefore consists of the KANMX (or HPHMX) dominant antibiotic resistance gene and the target gene homologous regions. This DNA product was introduced to the yeast cell by high efficiency transformation. KANMX (or HPHMX) integrates at the target locus, resulting in geneticin (or hygromycin) resistant transformants. The success of the knockout procedure was verified by PCR.

Droplet digital (dd)PCR

Yeast genomic DNA (gDNA) from each sample was isolated using the method described previously (Hoffman *et al.*, 1987). The concentration and purity of the DNA were determined using the NanoDrop 1000 spectrophotometer (Thermo Fisher Scientific Inc., Waltham, MA, USA) and restriction digested with the Sac1-HF (New England BioLabs inc., Ipswich, MA, USA). A final concentration of 0,1 ng digested DNA was used for the Droplet Digital Polymerase Chain Reaction (ddPCR). Unless otherwise stated, all the instruments, software, consumables, primers, and probes related to the ddPCR experiments were purchased from Bio-Rad Inc., Hercules, CA, USA. The mtDNA encoded cytochrome c oxidase subunit 3 (*COX3*) (SGD ID S000007283) gene, which encodes one of the three mtDNA subunits of complex IV of the mitochondrial electron transport chain, was used as a marker gene for the yeast mtDNA genome maintenance. A ddPCR

493 reaction probing the nuclear encoded gene *ACT1* (SGD ID S000001855) (encoding actin) was
494 used as a standard. *COX3* and actin gene-specific primers were labeled with HEX and FAM
495 probes respectively. The *COX3* primers sequences were: forward primer 5′-
496 CATTCAGCTATGAGTCCTG-3′, reverse primer 5′-CCTGCGATTAAGGCATG-3′ and Probe
497 sequence: 6HEX 5′-AGGTGCATGTTGACCACCCGTAGG-3′-lowa Black FQ. The *ACT1* primer
498 sequences were: forward primer 5′-CAAACCGCTGCTCAAT-3′, reverse primer 5′-
499 TACCTGGGAACATGGTG-3′, and the probe 6FAM-5′-
500 TGGTAACGAAAGATTCAGAGCCCCAGAAG-3′- lowa Black FQ. A T100™ Thermal Cycler
501 and the QX 200™ droplet reader were used and finally count of the positive and negative droplets
502 (events) utilizing the HEX/FAM channels was performed. The wells displaying ≥15000 events
503 were chosen for the analysis. QuantaSoft 1.7.4 software was used to analyses the copy number
504 variation (CNV). The reference gene was *ACT1* (one copy/haploid cell). CNV was expressed as
505 copies/cell. Three biological replicates were performed in the analysis.
506

507 **Mutagenesis and sectoring screen**

508 Ethylmethanesulfonate (EMS) mutagenesis was performed as described previously (Amberg *et*
509 *al.*, 2005). Yeast cultures were grown to an early stationary phase in SC selective medium
510 supplemented with 2% glucose. Two separate 1 ml samples (one as a control) were pelleted in a
511 table centrifuge (10 sec, 5000 g). The obtained pellets were washed once with distilled sterile
512 water and re-suspended in 0.1 M sodium phosphate buffer (pH 7.0). 30 µl of EMS were added to
513 one of the two tubes and mixed by vortexing. Both tubes were incubated for 50 min at 30˚C. Cells
514 were pelleted, re-suspended in 200 µl of 5% sodium thiosulfate, transferred to fresh tubes and
515 washed twice with 200 µl of 5% sodium thiosulfate, re-suspended in 1 ml of sterile water and

plated. 1:10-1:10000 dilutions from both the sample and the control (the cells incubated without EMS) were prepared for later calculation of the killing rate, which ranged between 50-80%. Petri dishes with cells plated on GSM medium were incubated at 30°C for 10-15 days. The sectoring screen was performed manually as described earlier (Kastaniotis *et al.*, 2004; Kursu *et al.*, 2013).

Cloning of the synthetic mutations

Upon loss of the *OM45* containing plasmid, it was not possible to complement the synthetic petite mutants with any plasmid encoding the intact copies of *OM45* or the mutated genes (our observation). For this reason, cloning by complementation had to be accomplished via two plasmid shuffles. First, the synthetic petite mutants carrying the pTSV30*OM45* plasmid were transformed with multicopy YEp112*OM45* (*TRP1* selective marker). Sectoring colonies obtained after the transformation were streaked out on SCG-TRP media containing 0.05% glucose. The white colonies collected from this re-streaking were further tested on SCD-LEU plates to confirm the loss of the pTSV30*OM45* plasmid. The *TRP1* marker allowed us to perform a counterselection against the *OM45* plasmid using 5-fluoroanthranilic acid (5-FAA) in the following step. For cloning of the mutations by complementation two multicopy libraries were used. pRS426-based (referred in the text as HeAl) (Kastaniotis *et al.*, 2004)was made in the Heitman laboratory by Clara Alarcon and contains yeast genomic sequences inserted in the *Sal*1 site of the vector and Lacroute library constructed by F. Lacroute in pFL44L (2μ plasmid with a URA3 marker) (Bonneaud *et al.*, 1991) with genomic DNA of strain FL100(Harington *et al.*, 1993).

Mutant strains carrying YEp112*OM45* were grown overnight on SCD-TRP media, transformed with the Lacroute or the HeAl library according to the High Efficiency lithium

538 acetate/SS-DNA/PEG protocol (Daniel Gietz *et al.*, 2002) and plated on SCG-URA plates
539 containing 250 mg/L 5-FAA, low tryptophan (10mg/L) and 0.05% glucose. Glucose was added in
540 this case to enhance the recovery of library transformants. The used concentration is low enough
541 to allow for efficient selection of the respiratory competent colonies.

542 **Test for petite colonies generation rate**

543 Strains from SCG plates grown overnight in liquid medium (YPD) were plated onto SCD and
544 SCG to yield in approximately 50-100 colonies per plate. After 7 days of incubation at 30˚C, the
545 colonies were replica plated onto YPD and SCG and incubated for 3-7 days at 30˚C. The number
546 of colonies on corresponding SCG (respiratory competent) and YPD (total number of colonies)
547 plates were determined. The number of the petite colonies = number of colonies on YPD plate
548 minus number of colonies on SCG plate.

549 **Construction of His6-Om45p, protein expression, purification and antibody production**

550 DNA encoding the soluble domain of Om45p without the first 22 amino acids (predicted N-
551 terminal transmembrane domain) was cloned onto the expression vector pET15b (Novagen-
552 Addgene, Cambridge, MA, USA) and expressed in *E. coli* BL21 (DE3). The expressed chimeric
553 protein containing a His6 tag on its N-terminus, a thrombin cleavage site and N-terminally
554 truncated Om45p was affinity purified with Ni^{2+} chelating Sepharose (GE Healthcare, Piscataway,
555 NJ, USA), concentrated 10 times with a Millipore Amicon Ultra-15 10000 NMWL concentrator
556 (Carrigtwohill, Cork, Ireland) in a table centrifuge at 4°C and subjected to anion-exchange
557 chromatography in Fractogel EMD DEAE (M) (Merck KGaA, Darmstadt, Germany), in a 10 x
558 150 mm column (20 mM Tris/HCl pH 7.4, a linear gradient elution with NaCl from 50 to 200 mM
559 at the flow rate 1 ml/min in 25 min). Purity of the peak fractions was controlled by SDS-PAGE

and mass spectrometry. Peak fractions were concentrated to 1.69 mg of protein per ml. 500 µl of the protein were used for generation of polyclonal antisera fin two rabbits by Davids Biotechnologie (Regensburg, Germany).

Fluorescence microscopy

Fluorescence microscopy was performed with either live or fixed cells using a Zeiss LSM700 confocal fluorescence microscope at 100x magnification. Mitochondria were visualized as described previously (Westermann *et al.*, 2000) with pYX142*mtGFP*, pVT100U*mtGFP* or using MitoTracker®Red CMX-ROS (Molecular Probes, Eugene, OR, USA). DAPI (Thermo Scientific, Rockford, IL, USA) staining of mtDNA in methanol-fixed cells was performed as described previously (Jones *et al.*, 1992).

Yeast cell fixation: For fixation, yeast cells were incubated in the growth media containing formaldehyde 4.4% (v/v) final concentration for 30 min at 30°C under shaking, then washed with 1.2 M sorbitol in 0.1 M $KHPO_4$ buffer (pH 6.5), harvested at 700 g for 1 min and stored at 4°C (Lee *et al.*, 1996).

Transmission electron microscopy

Transmission electron microscopy was performed according to the Tokuyasu method for yeast described previously (Griffith *et al.*, 2008). Cells were fixed in 2 % paraformaldehyde, 0.2 % glutaraldehyde in 0.1 M PHEM buffer (60 mM PIPES, 25 mM HEPES, 10 mM EGTA, 2 mM MgCl2, pH 6.9) at room temperature for 3 h. Cells were washed with 0.1M PHEM buffer,

resuspended in 1 % periodic acid in 0.1M PHEM buffer and incubated at room temperature for 1 h. After washing in 0.1M PHEM buffer, cells were infiltrated with 12 % gelatin dissolved in 0.1M PHEM buffer at 37ºC for 10 minutes. After solidification at 4ºC, small gelatin blocks were immersed in 2.3M sucrose and frozen in liquid nitrogen. Ultrathin (75 nm) sections were cut at -100 ºC using UC7 ultramicrotome with cryo attachement (Leica Microsystems) and picked up on grids with a drop of 1 % methyl cellulose, 1.1M sucrose mixture in PHEM buffer. Sections on a grid were contrasted with 2 % neutral uranyl acetate for 5 minutes, embedded in 2 % methyl cellulose, 0.4% uranyl acetate mixture and examined using Tecnai G2 Spirit transmission electron microscope (FEI Europe, Eindhoven, Netherlands). Images were captured by Quemesa CCD camera and analyzed using iTEM software (Olympus Soft Imaging Solutions, Münster, Germany). Yeast cell fixations and electron microscopy were performed by the staff of the Biocenter Oulu Electron microscopy core facility.

Lipid analysis

Preparation of the cells for lipid extraction: To prevent DNA loss during culture growth, yeast cell lawns were prepared on SCG plates supplemented with 2 mM ethanolamine (Etn) (Sigma-Aldrich), by incubation at 30°C for 4 days. The cells were scraped with 2 x 2 ml SCG containing Etn (or SCD containing Etn) media, inoculated in 400 ml SCG containing Etn (or SCD containing Etn) to OD_{595} 0.4 and grown for 43 h (or 15 h in case of SCD containing Etn).

For the phospholipidome analysis yeast cells were harvested from 400 ml growth culture by centrifugation. The cell mass was adjusted to 1 g wet weight, washed with sterile water. Cells were pelleted by centrifugation (5 min 3000 g), the pellets were frozen and stored at -70°C until lipid isolation.

Mitochondrial isolation for lipid extraction

Highly purified mitochondria were prepared as described before by Meisinger at al. (2000). Briefly, yeast cultures grown as described above were harvested by centrifugation (Beckman J-6-Mi) for 35 min at 5000 g, washed with deionized water and incubated for 20 min in DTT buffer [100 mM Tris/H_2SO_4 (pH 9.4), 10 mM DTT], 2 ml/g of wet cells, washed with zymolyase buffer [1.2 M sorbitol, 20 mM potassium phosphate buffer (pH 7.4)] and then digested with zymolyase 20T (5 mg/g of wet cells) in zymolyase buffer for 30 min. Spheroplasts were lysed in a Teflon potter (500 rpm) using 6.5 ml of homogenization buffer [(0.6 M sorbitol, 10 mM Tris/HCl, pH 7.4, 1 mM EDTA, 1 mM phenylmethylsulfonyl fluoride (PMSF), 0.2% (w/v)] per gram of wet cells. The homogenate was centrifuged at 1500 g for 5 min and the supernatant was further cleared by centrifugation at 3000 g for 5 min. The crude mitochondria from the supernatant were collected by centrifugation in SS-34 rotor at 12000 g for 15 min. The mitochondrial pellet was resuspended in cold SEM buffer (250 mM sucrose, 1 mM EDTA, 10 mM Mops, pH 7.2), manually homogenized in a small Teflon potter with 20 strokes, and centrifuged at 12000 g for 15 min. The pellets were resuspended in 5 ml of cold SEM buffer, applied to the sucrose gradient and ultracentrifuged at 100000 g for 30 min at 4°C. Mitochondria were collected with a syringe needle from the interface between the 32 and 64% sucrose layers. Mitochondria were washed with SEM buffer, weighed, flash frozen in liquid nitrogen in 200 µl of the SEM buffer and stored at -70°C.

The yeast samples for the lipid analysis were grown on synthetic complete media containing either glucose or glycerol, supplemented with 2 mM Etn. Etn supplementation was necessary since the negative control W1536 8B Δ*psd1*Δ*psd2* strain is an auxotroph for Etn.

Lipid extraction: Frozen cells (1 g) were thawed at room temperature and subjected to ethanol extraction (95% ethanol, 4 ml) in acid pre-washed glass tubes with a Teflon cover (Pyrex England) at 22˚C for 1 h under constant shaking (Vari-Mix, Barnstead/Thermolyne, Ashville, NC, USA). The standard lipids (1,2-diheptadecanoyl-sn-glycerol-3-phosphatidyl-ethanolamine m/z (-) 718.5387; 1,2-diheptadecanoyl-sn-glycerol-3-phosphatidyl-L-serine sodium salt m/z (-) 762.5292; 1,1,2,2-tetramyristol-cardiolipin (ammonium salt) m/z (-) 1239.841; L-α-lysophosphatidyl-choline-palmitoyl-D_3 (methyl-D_3) m/z (-) 557.36, each 0.2 µg/sample, were added to control the efficiency of the extraction. After 5 min spinning at 4100 g the supernatant was collected in a glass evaporation tube (vial no.1; Verex™. Phenomenex®, Torrance, CA, USA) and evaporated in a speed vac (ThermoElectron, SPD 2010, Ashville, NC, USA) at 45°C under vacuum. The pellets were further extracted twice for 20 min with 2 ml chloroform: methanol (2:1 v:v), centrifuged at 4000 g for 5 min after each extraction, and finally extracted twice in acidic solvent (20 min with 2 ml of chloroform: methanol: HCl (124:65:1 v:v:v) followed by centrifugation at 4000 g for 5 min after the acidity was adjusted to pH 4.0 with 0.5 M NaOH. Extracts from all steps were redissolved in 1 ml $CHCl_3$: methanol (2:1 v:v), combined and washed with 1 ml 0.9% NaCL of pH 3.0 (Christie WW, 2003).

Experiments with the lipids obtained from whole cells were performed in the following replicates: three independent experimental repeats were performed for each yeast strain; one to three independent repeats were taken from each sample culture. Two to three independent mass spectrometric measurements were performed from each lipid extraction. Overall, 13 measurements per yeast strain were performed for the determination of the phospholipid content in whole cells and six for the analysis of the mitochondrial phospholipidome.

LC-MS analysis: The separation of the phospholipids was performed on an UPLC® HSS T3 1.8 µm column (2.1 x 100 mm) at 55°C using an ultra-performance LC system (Waters Acquity™, Milford, MA, USA). The binary gradient was made with A: 10 mM ammonium acetate in acetonitrile and deionized water (60:40); B: 10 mM ammonium acetate in isopropanol/ acetonitrile (90:10). The column was eluted at 0.35 ml/min with a linear change from 60 to 100% B over 15 min.

Eluted lipids were analyzed by positive and negative electrospray ionisation in separate runs on a Synapt G-2 Quadrupole/time of flight mass spectrometer in MSE mode with lock mass correction over a mass range from 100 to 1500 Da.

Data were processed with Mass Lynx and its Marker Lynx option to obtain automatic quantification of large data sets. The ion counts were normalized to internal standards; lipids were identified by their accurate masses, MS/MS fragmentation, and their chromatographic behavior. The analysis was focused on the most abundant (C 34:2, C 34:1, C 32:2 and C 32:1) phospatidylserine (PS), phosphatidylethanolamine (PE), phosphatidylcholine (PC) and cardiolipin (CL) (CL 64:4; CL 66:4; CL 68:4; CL 70:4 and CL 72:4) species.

Protein analysis

Protein extraction for western blot analysis: Proteins were extracted from the cultured yeast cells or directly from the plate lawns as described previously by Platta et. al. 2004 (Platta *et al.*, 2004). In brief, cells were harvested by centrifugation, washed with sterile water. 30 mg of cell pellets and mixed with 15 µl of 1 M potassium phosphate buffer, pH 7.4 and 100 µL of trichloroacetic acid were incubated for 30 min at -70˚C, thawed and pelleted. Proteins were further precipitated in 500 µl of ice-cold 80% acetone, pelleted, re-dissolved in 60 µl of 1% SDS/0.1 M

668 NaOH and 20 µl of 4 x SDS loading buffer [500mM Tris/Cl (pH 6.8), 10% SDS, 30% glycerol,
669 bromphenolblue, 10% β-mercaptoethanol], heated 5 min at 95˚C.

670 **SDS-PAGE and western blot analysis:** Proteins were analyzed by SDS-PAGE (12%) (Laemmli,
671 1970), stained with Coomassie brilliant blue or subjected to Western blotting using nitrocellulose
672 membranes (Bio-Rad) and the enhanced chemiluminescence system (Bio-Rad).

673

ACKNOWLEDGEMENTS

We thank Päivi Joensuu for technical assistance in the phospholipid analysis, Dr. A-M Escobar-Henriques Dias and Prof. J. Riemer for discussions and valuable suggestions. This work was carried out at the Faculty of Biochemistry and Molecular Medicine and Biocenter Oulu of the University of Oulu, Finland.

AUTHOR CONTRIBUTIONS

TS planned the experiments, carried out the experimental work, wrote the article and generated the Figures. AJM did additional experimental work, generated figures and participated in writing of the article. LS, UB, GM and IJM carried out experiments, analyzed data and contributed to the writing process. JKH planned experiments and participated in the writing of the article. AJK planned experiments, supervised the work and participated in the writing of the article.

687 GRAPHICAL ABSTRACT

688

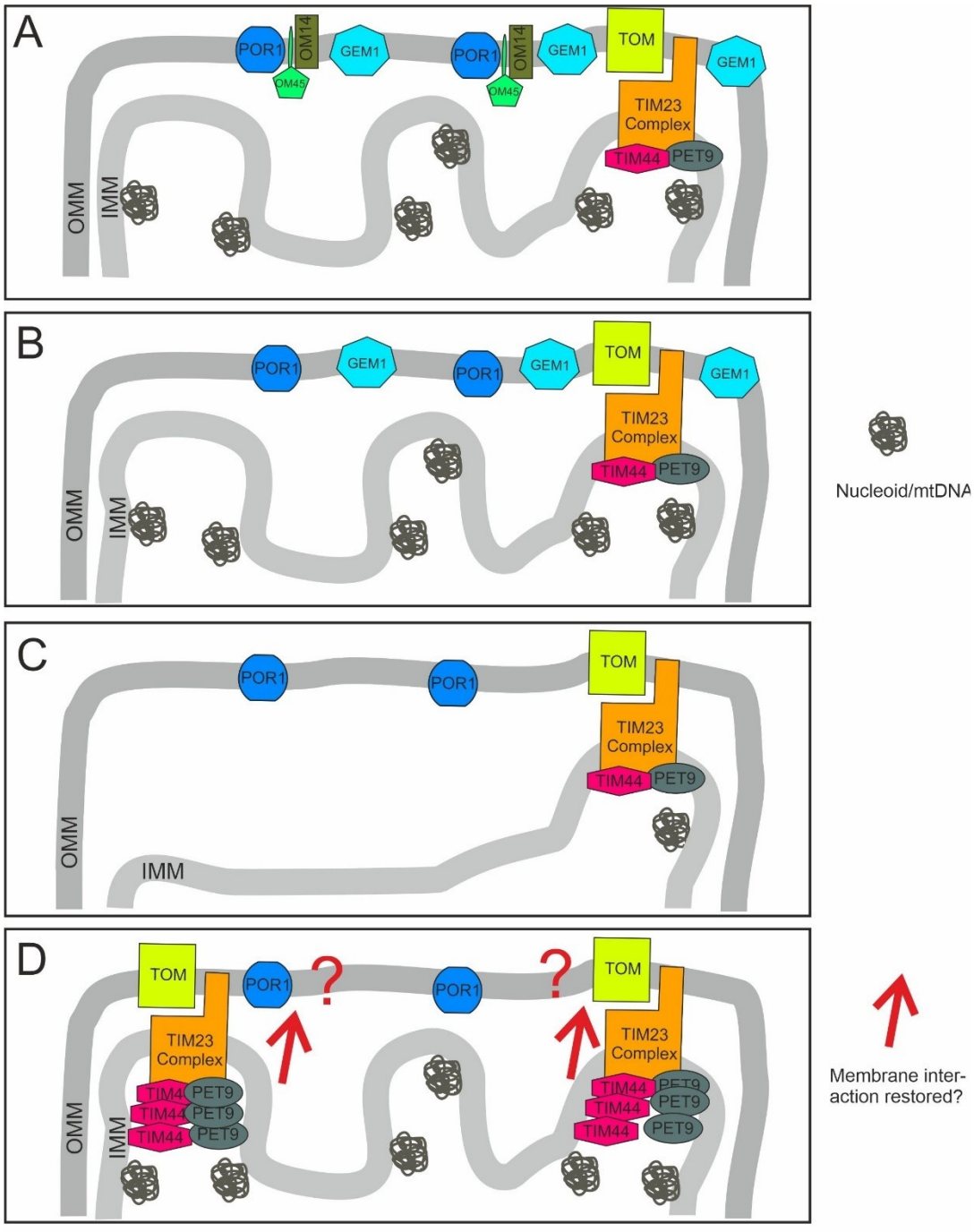

Graphical abstract Shvetsova *et al*. **A.** WT state. **B.** In the Δ*om45* strain has no detectable phenotype. **C.** The Δ*om45,* Δ*gem1* synthetic petite (SPM) strain is respiratory deficient, displays severely disturbed IMM morphology and loss of mitochondrial DNA. **D.** Overexpression of several factors, many of them involved in TIM function or respiratory chain assembly alleviates the mitochondrial defects and presumably the IMM morphology defect in the SPM strain. The mechanism how mitochondrial function is restored is not clear. Increased IMM/OMM interaction unrelated to Gem1/Om45 function may play a role. OMM: Outer mitochondrial membrane. IMM: Inner mitochondrial membrane

FUNDING INFORMATION

Financial support was provided by Biocenter Oulu, the Academy of Finland and the Sigrid Jusélius Foundation.

ETHICS APPROVAL STATEMENT

No animals or humans were subjects of these studies.

ABBREVIATED SUMMARY

A screen in *Saccharomyces cerevisiae* for mutations that are synthetically respiratory deficient with a deletion of the *OM45* gene, encoding a major yeast mitochondrial outer membrane protein, led to the isolation of mutations in the *UGO1* and *GEM1*. Our results indicate the inner mitochondrial membrane (IMM) as the location of action of Om45 and the Miro GTPase Gem1, and a role for these proteins in maintenance of IMM morphology and mitochondrial DNA.

701 **TABLE 1** Yeast strains used in this study

Plasmid	Reference	Yeast marker
pAG32	(Goldstein et al., 1999)	*HPHMX*
pET 15b	Novagen	*E.coli* expression vector
pET 15b*OM45*	This study	*E.coli* expression vector
pTSV30A	generated by J. Pringle and M. Longtine, previously described (Kastaniotis et al., 2004)	*LEU2*
pTSV30*OM45*	This study	*LEU2*
pVT100U mt*GFP*	(Westermann et al., 2000)	*URA3*
pYM8	(Knop et al., 1999).	*KanMX*
YCp22*FZO1*	This study	*TRP1*
YCp22*UGO1*	This study	*TRP1*
YCp22*ugo1-1*(P189L)	This study	*TRP1*
YCp33*ADH1*	This study	*URA3*
YCp33*ADH1*prom	This study	*URA3*
YCp33*ADH*prom*OM45*(own terminator)	This study	*URA3*
YCp33*AIM2*	This study	*URA3*
YCp33*AIM2*	This study	*URA3*
YCp33*DNM1*	This study	*URA3*
YCp33*FZO1*	This study	*URA3*
YCp33*GEM1*	This study	*URA3*
YCp33*gem1-1*(R103K))	This study	*URA3*
YCp33*gem1-2*(S324N)	This study	*URA3*
YCp33*MSC1*	This study	*URA3*
YCp33*OM45*	This study	*URA3*
YCp33*OM451GFP*	This study	*URA3*
YCp33*PET54*	This study	*URA3*
YCp33*PET9*	This study	*URA3*
YCp33*PRP3*	This study	*URA3*
YCp33*RPL27b*	This study	*URA3*
YCp33*RTT109*	This study	*URA3*
YCp33*SHY1*	This study	*URA3*

Plasmid	Reference	Yeast marker
YCp33*TIM44*	This study	*URA3*
YCp33*UGO1*	This study	*URA3*
YCp33*YGR111*	This study	*URA3*
YCp33*YOR228c*	This study	*URA3*
YCplac111	(Gietz et al. 1988)	*LEU2*
YCplac22	(Gietz et al. 1988)	*LEU2*
YCplac33	(Gietz et al. 1988)	*URA3*
YEp112*FZO1*	This study	*TRP1*
YEp112*OM45*	This study	*TRP1*
YEp112*UGO1*	This study	*TRP1*
YEp112*ugo1-1*(P189L)	This study	*TRP1*
YEp181*OM45*-proA	This study	*URA3*
YEp195*ADH1*prom*OM45*	This study	*URA3*
YEp195*AIM2*	This study	*URA3*
YEp195*AIM2*	This study	*URA3*
YEp195*DNM1*	This study	*URA3*
YEp195*FZO1*	This study	*URA3*
YEp195*FZO1*	This study	*URA3*
YEp195*GEM1*	This study	*URA3*
YEp195*OM45*	This study	*URA3*
YEp195OM45GFP	This study	*URA3*
YEp195*OM45-GFP*	This study	*URA3*
YEp195*PET54*	This study	*URA3*
YEp195*PRP3*	This study	*URA3*
YEp195*RTT109*	This study	*URA3*
YEp195*SHY1*	This study	*URA3*
YEp195*TIM44*	This study	*URA3*
YEp352(CTA1)OM45	This study	*URA3*
YEplac112	(Gietz et al. 1988)	*TRP1*
YEplac181	(Gietz et al. 1988)	*URA3*
YEp*lac*195	(Gietz et al. 1988)	*URA3*

Plasmid	Reference	Yeast marker

TABLE 2

Yeast strains used in this study

Name	Genotype	Reference of the source
W1536 8B	*MAT α ade2Δ, ade3Δ, can1-100, his3-1115, leu2-3112, trp1-1,ura3-1*	(Kastaniotis *et al.*, 2004)
W 1536 8B Δ*om45*	MAT α *ade2Δ, ade3Δ, can1-100, his3-1115, leu2-3112, trp1-1,ura3-1, yil136w::KanMX4*	This study
W 1536 8B Δ*gem1*	MAT α *ade2Δ, ade3Δ, can1-100, his3-1115, leu2-3112, trp1-1,ura3-1, yal048c::HPHMX*	This study
W 1536 8B Δ*gem1*Δ*om45*	MAT α *ade2Δ, ade3Δ, can1-100, his3-1115, leu2-3112, trp1-1,ura3-1, yil136w::KanMX4, yal048c::HPHMX*	This study
W1536 8B Δ*om45* Δ*ugo1*	MAT α *ade2Δ, ade3Δ, can1-100, his3-1115, leu2-3112, trp1-1,ura3-1, yil136w::KanMX4,Δydr470c::HPH MX4*	This study
W1536 8B Δ*psd2*	MAT α *ade2Δ, ade3Δ, can1-100, his3-1115, leu2-3112, trp1-1,ura3-1;psd2::ClonNat*	This study
W1536 8B Δ*psd1*Δ*psd2*	MAT α *ade2Δ, ade3Δ, can1-100, his3-1115, leu2-3112, trp1-1,ura3-1; psd2::ClonNat; ynl169c::HPH MX*	This study
W 1536 8B Δ*gem1*Δ*om45*Δ*psd2*	MAT α *ade2Δ, ade3Δ, can1-100, his3-1115, leu2-3112, trp1-1,ura3-1, yil136w::KanMX4, yal048c::HPHMX, psd2::ClonNat*	This study
W 1536 8B Δ*om45* Δ*psd2*	MAT α *ade2Δ, ade3Δ, can1-100, his3-1115, leu2-3112, trp1-1,ura3-1, yil136w::KanMX4, psd2::ClonNat*	This study
W 1536 8B Δ*gem1* Δ*psd2*	MAT α *ade2Δ, ade3Δ, can1-100, his3-1115, leu2-3112, trp1-1,ura3-1, yal048c::HPHMX, psd2::ClonNat*	This study

FIGURE LEGENDS

Figure 1. Synthetic petite screen in yeast hunting for genetic interactions of *OM45*. A. Schematic outline of the screen. W1536 5B/8B strains carrying an *ade2, ade3* double deletion, as well as *leu2, ura3* and *trp1* marker mutations are deleted for *om45* (Δ*om45*). When transformed with the pTSV30*OM45* plasmid carrying *OM45* and *ADE3* genes (as well as the *LEU2* gene as a transformation selection marker), the cells become genotypically Δ*ade2* and develop the characteristic red colony color phenotype. Without selection for the plasmid, it is lost at high frequency, resulting in a "sectored" colony color appearance. The cells are exposed to the mutagen ethylmethane sulfonate (EMS) and plated on media containing only a non-fermentable carbon source. Synthetic petite mutants are identified by their inability to lose the *OM45* plasmid on non-fermentable media, which can be monitored by formation of completely red, non-sectoring colonies on synthetic complete glycerol (SCG) media. Ability to lose the OM45 plasmid on synthetic complete dextrose (glucose) (SCD) media indicates that the mutation only affects mitochondrial function, but not respiratory growth. **SPM** synthetic petite mutant. The **X** symbolizes the mutation in an interacting gene. B. and C**.** Test for dependence of SPMs on the *OM45* plasmid for respiratory growth and demonstration of respiratory deficiency in absence of *OM45*. B. The synthetically petite mutant *gem1(R103K)* and C. *ugo1(P189L)* obtained via the genetic screens are respiratory deficient upon loss of the *OM45* plasmid. All the complementation studies were done via plasmid shuffle, loss of the original pTSV30*OM45* plasmid was monitored *via* colony sectoring and confirmed by re-streaking on SC-LEU drop-out media supplemented with

glucose. Only strains that carry a copy of *OM45* on a plasmid are viable on respiratory media (SCG). All strains are able to grow on media containing the fermentable carbon source glucose (SCD, lowest panel). D. Schematic representation of the location of the obtained synthetic mutations in the Gem1 and Ugo1 translation products based on published data on Ugo1 (J Cell Biol (2009) 184 (4): 569–581.) (Hoppins *et al.*, 2009) and Gem1 (J Cell Biol. 2004 Oct 11; 167(1): 87–98.) (Frederick *et al.*, 2004) Black boxes designate transmembrane domains (TMDs). MIRO: GTPase domains; EF1/2: EF-hand domains. E. Nucleotide and amino acid sequences of obtained synthetic petite mutations. The sequence excerpt encoding the *gem1*(R103K) and *gem1*(S324N) mutations shows nucleotides 301-324 and 961-984 of the *GEM1* ORF, respectively. The *UGO1* ORF sequence excerpt stretches from 553-576. Mutated amino acid residues and corresponding wild type residues are marked in red.

Figure 2. Synthetic lethal mutants show mitochondrial morphology defects in the absence of the complementing *OM45* plasmid.

Yeast cells from wild-type (WT), SPMs and SPMs with the complementing plasmid were grown in selective liquid synthetic complete medium supplemented with glucose (2%) to mid-log phase, and mitochondria (Mito) were visualized by mitochondria-targeted GFP. The *om45* deletion does not visibly affect mitochondrial morphology (second row from the top). The *gem1* mutants still maintain some tubular structure but display mitochondrial fragmentation and collapsed structure (rows three and four from the top). This phenotype is exacerbated in the *ugo1* SPM, which nearly completely lacks long tubular mitochondria. Mitochondrial morphology of the SPM cells is rescued by presence of a plasmid-borne copy of *OM45*, here shown for the Δ*om45,ugo1*(P198L) SPM. BR: brightfield image; Mito: mitochondrially

751 targeted GFP. Projection images of mitochondria were generated using the Zeiss software (see
752 Materials and Methods). Size bar: 5µm.
753
754 **Figure 3.** Quantitative analysis of mitochondrial morphology types in SPM cells in absence
755 or presence of complementing *OM45*. A. Representative images of morphology types
756 observed in W1536 8B Δ*gem*1Δ*om45* cells with and without the complementing 2µ
757 OM45plasmid. Mitochondria were visualized using matrix targeted mtGFP expressed from
758 the pVT100U mtGFP (*URA3*) plasmid. Cells were grown overnight in selective liquid
759 synthetic complete medium supplemented with glucose (2%). B. Quantification of
760 mitochondrial morphology phenotypes as exemplified in panel A. Shown are % ratios of cells
761 from 3 experimental replicates observing at least 100 cells in each experiment are shown.
762
763 **Figure 4**. Inner mitochondrial membrane folding is distorted in synthetic petite mutants upon
764 loss of the *OM45* plasmid.
765 Electron micrographs of the synthetic petite mutants (A, C, E) with pTSV30*OM45* and (B, D,
766 F) without pTSV30*OM45*. The *gem1* synthetic petites (B and D) show clear improvement of
767 cristae structure in presence of the *OM45* carrying plasmid (A and C). The *ugo1* mutant,
768 which has highly disturbed mitochondrial membrane structure (F), also shows mitochondria
769 with a more regular shape in presence of *OM45* (E). Arrows point at mitochondria. Cells were
770 grown o/n in liquid synthetic complete media supplemented with glucose (2%). Arrows
771 indicate mitochondria. Scale bar 200 nm.
772

773 **Figure 5.** Growth phenotypes of reconstructed SPMs, mitochondrial morphology changes and
774 mtDNA loss of the W1536 8B Δ*om45*Δ*gem1* strain.
775 A. The Δ*om45*Δ*gem1* strain exhibits a synthetic petite phenotype, already apparent from the
776 slow growth on SCD media. The SPM-derived *gem1* mutant alleles only partially rescue
777 growth in comparison to WT *GEM1*. Yeast strains were grown overnight in appropriate SC or
778 SC selective liquid medium supplemented with glycerol. Cultures were normalized to
779 OD595=1.0 and serial 10-fold dilutions were spotted onto SC solid media supplemented with
780 glucose (2%) or glycerol (3%). Photographs were taken after 3 and 5 days of growth at 30°C
781 for yeast growing in glucose and glycerol media, respectively. B. Electron micrograph of
782 W1536 8B Δ*om45*Δ*gem1* with similarly disturbed cristae structure as the SPMs in Fig. 4. C.
783 the same strain carrying the 2μ*OM45* plasmid, with improved cristae structure. Cells were
784 grown for 4 days in liquid synthetic complete media supplemented with glycerol (3%). EM
785 Scale bar: 500 nm.
786 D. Electron micrograph of WT strain W1536 8B mitochondria**.** Scale bar indicates 500 nm. E.
787 Scheme for testing the rate of petite formation. After prolonged growth on fermentable media,
788 the Δ*gem1* strain exhibits a mild increase of the respiratory deficient fraction of cells, while
789 the Δ*om45*Δ*gem1* double mutant massively accumulates respiratory deficient cells. Strains
790 were initially grown on SCG media. They were then inoculated in liquid SC media
791 supplemented with glucose (2%), grown overnight, and plated on solid rich YP media
792 supplemented with glucose (2%). After 7 days incubation at 30˚C colonies were counted, and
793 replica plated on solid SC media supplemented with glycerol (3%). The number of the petite
794 colonies = number of colonies on YPD plate minus number of colonies on SCG plate (N=3).
795 F. Statistical representation of experiment described in (E). G. ddPCR analysis of mtDNA

content in cells grown on glucose or Glycerol. All the yeast strains were transferred from a SCG plate on a YPD (2% glucose) plate (mother plate). Individual colonies from the mother plate were re-streaked on YPD plates several times and checked on the YPG plate for respiration competence. For genomic DNA isolation, all the strains were grown on YPD (2% glucose) liquid media overnight. Negative control: BY4741Δ*mtf2*

Figure 6. Complementation potency of Om45 is diminished by C-terminal GFP tagging.
Spotting assay with the A. W1536 8B Δ*om45*Δ*gem1* and B. W1536 8B Δ*om45* strain expressing Om45 or Om45-GFP from *CEN* (*URA3*) or 2µ (*URA3*) (multicopy) plasmids. Yeast strains carrying an indicated plasmid were grown overnight in synthetic complete medium lacking uracil and supplemented with glycerol (3%). Cultures were normalized to OD_{595}=1.0 and serial 10-fold dilutions were spotted onto synthetic complete solid media lacking uracil and supplemented with either glucose (2%) or glycerol (3%). Photographs were taken after 3 and 5 days of growth at 30°C for yeast growing in glucose and glycerol media, respectively. C. Representative western blot image. Om45-GFP levels expressed in Δom45 are comparable to Om45p levels expressed from the corresponding vector. Cells were grown at 30°C. Western blot probed with anti-OM45p rabbit serum and anti-rabbit antibodies conjugated to HRP. Imaging with BioRad ChemiDoc™.
D. SPM complementation with *CEN* and 2µ *OM45* plasmids. Cells carrying a 2µ *OM45*(*TRP1*) plasmid and either of the test plasmids were plated on SCG-URA low TRP medium supplemented with 5'FAA for *TRP1* plasmid counterselection. *OM45*-GFP (*CEN*)

818 (low copy plasmid); *OM45*-GFP (2μ) (high copy plasmid); YCp33*OM45* (+); YCp*lac*33 (-)
819 (empty plasmid).
820
821 **Supplementary Figure 1.** Growth phenotype of W1536 8B wild type and om45 deletion
822 strain on different growth media.
823 Yeast strains were grown overnight in SC liquid medium supplemented with glucose. Cultures
824 were normalized to OD_{595}=1.0 and serial 10-fold dilutions were spotted onto corresponding
825 solid media. Photographs were taken after 3 -6 days of growth.
826
827 **Supplementary Figure 2.** Tetrad dissection of SPMs. Cells were initially dissected on YPD
828 or SCD media and then replica plated on the indicated selective media (SCG and SCLac or
829 only SCG). The Δ*om45, ugo1(P198L)* examples show the dissection master plate before
830 transfer, the other examples the SCD master plate AFTER replica plating/transfer.
831
832 **Supplementary figure 3.** Growth of the reconstructed of Δom45/ugo1 SPM.
833 Strains were constructed in a similar manner as the reconstructed *gem1* SPMs (BY series
834 background), initially generating the Δ*om45,* Δ*ugo1* double deletion mutant. However, a
835 plasmid harboring WT *UGO1* was maintained throughout to prevent mitochondrial DNA loss.
836 The reconstructed SPM has a mild growth defect in this strain background, indicating partial
837 function of the *ugo1(P189L)* – encoded protein. Presence of *UGO1* in the Δ*om45,*
838 Δ*ugo1*mutant completely rescued growth and presence of both plasmids carrying the
839 *ugo1(P189L)* mutant allele and *OM45* improved growth compared to the *ugo1(P189L)*
840 construct being present alone, albeit not completely to WT levels on glycerol. When the

841 Δ*om45, Δugo1* mutant strain only carried empty plasmids, the cells were completely
842 respiratory deficient.
843
844 **Supplementary Figure 4.** Mitochondrial morphology changes and mtDNA loss in the SPM.
845 Representative images of morphology types observed in W1536 8B WT, W1536 8B Δom45
846 and SPM cells with and without the complementing 2μ OM45plasmid. Mitochondria
847 visualization was done with matrix targeted mtGFP expressed from plasmid pVT100U
848 mtGFP(*URA3*). Cells were grown overnight in selective liquid synthetic complete medium
849 supplemented with glucose (2%). mtDNA was visualized with DAPI stain.
850 Concentration of mtDNA determined with ddPCR in the mutants with and without 2μ *OM45*
851 plasmid grown over night on SC or SC selective medium supplemented with 2% glucose.
852
853 **Supplementary Figure 5.** Growth assay of the W1536 8BΔom45, ugo1(P189L) mutant
854 transformed with multicopy suppressor plasmids
855
856 **Supplementary Figure 6.** Growth assay of the W1536 8BΔom45, gem1(R103K) mutant
857 transformed with multicopy suppressor plasmids
858
859 **Supplementary Figure 7.** Whole cell and mitochondrial phospholipidome analysis of W1536
860 8B Δ*psd2,* W1536 8B Δ*psd2*Δ*om45*, W1536 8B Δ*psd2*Δ*gem1*, W1536 8BΔ*psd2*Δ*om45*Δ*gem1*
861 and W1536 8B Δ*psd2*Δ*psd1* strains. A. Cellular content of indicated phospholipids from total
862 cells phospholipid preparations in the indicated yeast strains. B. Ratio of phosphatidylserine
863 over phosphatidylethanolamine from total cell phospholipids. C. Mitochondrial content of

total cells phospholipid preparations in the indicated yeast strains. D. Ratio of phosphatidylserine over phosphatidylethanolamine from mitochondrial phospholipids preparations. CL: cardiolipin; PE: phosphatidylethanolamine; PS: phosphatidylserine; PC: phosphatidylcholine.

Phospholipids were extracted either from whole cells grown on SCG, or from mitochondria purified from cells grown on SCG. The pictures present % ratios, with the total sample phospholipids set as100%. The statistically supported changes as indicated with * between the samples and W 1536 8B Δ*psd2* control ($p<0.05$), **($p<0.01$) were determined with a t-test (two-tailed, paired).

REFERENCES

Abrams, A.J., Hufnagel, R.B., Rebelo, A., Zanna, C., Patel, N., Gonzalez, M.A.*, et al.* (2015) Mutations in SLC25A46, encoding a UGO1-like protein, cause an optic atrophy spectrum disorder. *Nat Genet*.

Alkhaja, A.K., Jans, D.C., Nikolov, M., Vukotic, M., Lytovchenko, O., Ludewig, F.*, et al.* (2012) MINOS1 is a conserved component of mitofilin complexes and required for mitochondrial function and cristae organization. *Mol Biol Cell* **23:** 247-257.

Amberg, D.C., Burke, D.J., and Strathern, J.N. (2005) Methods in Yeast Genetics: A Cold Spring Harbor Laboratory Course Manual, 2005 Edition (Cold Spring).

Anton, F., Fres, J.M., Schauss, A., Pinson, B., Praefcke, G.J.K., Langer, T., and Escobar-Henriques, M. (2011) Ugo1 and Mdm30 act sequentially during Fzo1-mediated mitochondrial outer membrane fusion. *J Cell Sci* **124:** 1126-1135.

Ausubel, F., Brent, R., Kingston, R., Moore, D., Seidman, J., and Smith, J. (1989) StruhlK (Eds): Current Protocols in Molecular Biology.

Blom, J., Kubrich, M., Rassow, J., Voos, W., Dekker, P.J., Maarse, A.C., *et al.* (1993) The essential yeast protein MIM44 (encoded by MPI1) is involved in an early step of preprotein translocation across the mitochondrial inner membrane. *Mol Cell Biol* **13:** 7364-7371.

Bonneaud, N., Ozier−Kalogeropoulos, O., Li, G., Labouesse, M., Minvielle−Sebastia, L., and Lacroute, F. (1991) A family of low and high copy replicative, integrative and single−stranded S. cerevisiae/E. coli shuttle vectors. *Yeast* **7:** 609-615.

Burri, L., Vascotto, K., Gentle, I.E., Chan, N.C., Beilharz, T., Stapleton, D.I., *et al.* (2006) Integral membrane proteins in the mitochondrial outer membrane of Saccharomyces cerevisiae **273:** 1507-1515.

Carman, G.M., and Henry, S.A. (1999) Phospholipid biosynthesis in the yeast< i> Saccharomyces cerevisiae</i> and interrelationship with other metabolic processes. *Prog Lipid Res* **38:** 361-399.

Chen, D., Yang, B., and Kuo, T. (1992) One-step transformation of yeast in stationary phase. *Curr Genet* **21:** 83-84.

Christie WW (2003) *Lipid analysis. isolation, separation, identification and structural analysis of lipids*: The Oily Press.

Coonrod, E.M., Karren, M.A., and Shaw, J.M. (2007) Ugo1p Is a Multipass Transmembrane Protein with a Single Carrier Domain Required for Mitochondrial Fusion. *Traffic* **8:** 500-511.

Gietz R.D., and Woods, R.A. (2002) Transformation of yeast by lithium acetate/single-stranded carrier DNA/polyethylene glycol method. *Meth Enzymol* **350:** 87-96.

Gietz R.D., and Sugino A. (1988). New yeast Escherichia coli shuttle vectors constructed with in vitro mutagenized yeast genes lacking six-base pair restriction sites. *Gene* 74:527-534.

Daum, G., and Vance, J.E. (1997) Import of lipids into mitochondria. *Prog Lipid Res* **36:** 103-130.

D'Silva, P., Liu, Q., Walter, W., and Craig, E.A. (2004) Regulated interactions of mtHsp70 with Tim44 at the translocon in the mitochondrial inner membrane **11:** 1084-1091.

Frederick, R.L., McCaffery, J.M., Cunningham, K.W., Okamoto, K., and Shaw, J.M. (2004) Yeast Miro GTPase, Gem1p, regulates mitochondrial morphology via a novel pathway. *J Cell Biol* **167:** 87-98.

Goldstein, A.L., and McCusker, J.H. (1999) Three new dominant drug resistance cassettes for gene disruption in Saccharomyces cerevisiae. *Yeast* **15:** 1541-1553.

Griffith, J., Mari, M., De Mazière, A., and Reggiori, F. (2008) A cryosectioning procedure for the ultrastructural analysis and the immunogold labelling of yeast *Saccharomyces cerevisiae.*

Traffic **9:** 1060-1072.

Harington, A., Herbert, C., Tung, B., Getz, G., and Slonimski, P. (1993) Identification of a new nuclear gene (CEM1) encoding a protein homologous to a β−keto−acyl synthase which is essential for mitochondrial respiration in Saccharomyces cerevisiae. *Mol Microbiol* **9:** 545-555.

Harner, M., Korner, C., Walther, D., Mokranjac, D., Kaesmacher, J., Welsch, U.*, et al.* (2011) The mitochondrial contact site complex, a determinant of mitochondrial architecture. *EMBO J* **30:** 4356-4370.

Hoffman, C.S., and Winston, F. (1987) A ten-minute DNA preparation from yeast efficiently releases autonomous plasmids for transformaion of Escherichia coli. *Gene* **57:** 267-272.

Hoppins, S., Collins, S.R., Cassidy-Stone, A., Hummel, E., DeVay, R.M., Lackner, L.L.*, et al.* (2011) A mitochondrial-focused genetic interaction map reveals a scaffold-like complex required for inner membrane organization in mitochondria. *J Cell Biol* **195:** 323-340.

Hoppins, S., Horner, J., Song, C., McCaffery, J.M., and Nunnari, J. (2009) Mitochondrial outer and inner membrane fusion requires a modified carrier protein. *J Cell Biol* **184:** 569-581.

Horvath, S.E., and Daum, G. (2013) Lipids of mitochondria. *Prog Lipid Res* **52:** 590-614.

Itoh, K., Tamura, Y., Iijima, M., and Sesaki, H. (2013) Effects of Fcj1-Mos1 and mitochondrial division on aggregation of mitochondrial DNA nucleoids and organelle morphology. *Mol Biol Cell* **24:** 1842-1851.

Jones, B.A., and Fangman, W.L. (1992) Mitochondrial DNA maintenance in yeast requires a protein containing a region related to the GTP-binding domain of dynamin. *Genes Dev* **6:** 380-389.

Kanki, T., Kang, D., and Klionsky, D.J. (2009) Monitoring mitophagy in yeast. *Autophagy* **5:** 1186-1189.

Kastaniotis, A.J., Autio, K.J., Sormunen, R.T., and Hiltunen, J.K. (2004) Htd2p/Yhr067p is a yeast 3-hydroxyacyl-ACP dehydratase essential for mitochondrial function and morphology. *Mol Microbiol* **53:** 1407-1421.

Knop, M., Siegers, K., Pereira, G., Zachariae, W., Winsor, B., Nasmyth, K., and Schiebel, E. (1999) Epitope tagging of yeast genes using a PCR−based strategy: more tags and improved practical routines. *Yeast* **15:** 963-972.

Kornmann, B., Osman, C., and Walter, P. (2011) The conserved GTPase Gem1 regulates endoplasmic reticulum-mitochondria connections. *Proc Natl Acad Sci U S A* **108:** 14151-14156.

Kursu, V.A.S., Pietikäinen, L.P., Fontanesi, F., Aaltonen, M.J., Suomi, F., Raghavan Nair, R.*, et al.* (2013) Defects in mitochondrial fatty acid synthesis result in failure of multiple aspects of mitochondrial biogenesis in Saccharomyces cerevisiae. *Mol Microbiol* **90:** 824-840.

Laemmli, U.K. (1970) Cleavage of structural proteins during the assembly of the head of bacteriophage T4. *Nature* **227:** 680-685.

Lauffer, S., Mabert, K., Czupalla, C., Pursche, T., Hoflack, B., Rodel, G., and Krause-Buchholz, U. (2012) Saccharomyces cerevisiae Porin Pore Forms Complexes with Mitochondrial Outer Membrane Proteins Om14p and Om45p. *J Biol Chem* **287:** 17447-17458.

Lee, M.S., Henry, M., and Silver, P.A. (1996) A protein that shuttles between the nucleus and the cytoplasm is an important mediator of RNA export. *Genes Dev* **10:** 1233-1246.

Linden, A., Deckers, M., Parfentev, I., Pflanz, R., Homberg, B., Neumann, P.*, et al.* (2020) A Cross-linking Mass Spectrometry Approach Defines Protein Interactions in Yeast Mitochondria. *Mol Cell Proteomics* **19:** 1161-1178.

Liu, Q., Krzewska, J., Liberek, K., and Craig, E.A. (2001) Mitochondrial Hsp70 Ssc1: role in protein folding. *J Biol Chem* **276:** 6112-6118.

Mannella, C.A. (1992) The 'ins' and 'outs' of mitochondrial membrane channels. *Trends Biochem Sci* **17:** 315-320.

McMaster, C.R. (2018) From yeast to humans–roles of the Kennedy pathway for phosphatidylcholine synthesis. *FEBS Lett* **592:** 1256-1272.

Nguyen, T.T., Lewandowska, A., Choi, J., Markgraf, D.F., Junker, M., Bilgin, M.*, et al.* (2012) Gem1 and ERMES do not directly affect phosphatidylserine transport from ER to mitochondria or mitochondrial inheritance. *Traffic* **13:** 880-890.

Ohlmeier, S., Kastaniotis, A.J., Hiltunen, J.K., and Bergmann, U. (2004) The Yeast Mitochondrial Proteome, a Study of Fermentative and Respiratory Growth. *J Biol Chem* **279:** 3956-3979.

Pfanner, N., Douglas, M.G., Endo, T., Hoogenraad, N.J., Jensen, R.E., Meijer, M.*, et al.* (1996) Uniform nomenclature for the protein transport machinery of the mitochondrial membranes. *Trends Biochem Sci* **21:** 51-52.

Pfanner, N., van der Laan, M., Amati, P., Capaldi, R.A., Caudy, A.A., Chacinska, A.*, et al.* (2014) Uniform nomenclature for the mitochondrial contact site and cristae organizing system. *J Cell Biol* **204:** 1083-1086.

Platta, H., Girzalsky, W., and Erdmann, R. (2004) Ubiquitination of the peroxisomal import receptor Pex5p. *Biochem J* **384:** 37-45.

Popov−Čeleketić, D., Mapa, K., Neupert, W., and Mokranjac, D. (2008) Active remodelling of the TIM23 complex during translocation of preproteins into mitochondria. *EMBO J* **27:** 1469-1480.

Rabl, R., Soubannier, V., Scholz, R., Vogel, F., Mendl, N., Vasiljev-Neumeyer, A.*, et al.* (2009) Formation of cristae and crista junctions in mitochondria depends on antagonism between Fcj1

and Su e/g. *J Cell Biol* **185:** 1047-1063.

Riezman, H., Hay, R., Gasser, S., Daum, G., Schneider, G., Witte, C., and Schatz, G. (1983) The outer membrane of yeast mitochondria: isolation of outside-out sealed vesicles. *EMBO J* **2:** 1105-1111.

Sesaki, H., and Jensen, R.E. (2001) UGO1 encodes an outer membrane protein required for mitochondrial fusion. *J Cell Biol* **152:** 1123-1134.

Sesaki, H., and Jensen, R.E. (2004) Ugo1p links the Fzo1p and Mgm1p GTPases for mitochondrial fusion. *J Biol Chem* **279:** 28298-28303.

Sesaki, H., Southard, S.M., Yaffe, M.P., and Jensen, R.E. (2003) Mgm1p, a dynamin-related GTPase, is essential for fusion of the mitochondrial outer membrane. *Mol Biol Cell* **14:** 2342-2356.

Song, J., Tamura, Y., Yoshihisa, T., and Endo, T. (2014) A novel import route for an N−anchor mitochondrial outer membrane protein aided by the TIM23 complex. *EMBO Rep*.

Stone, S.J., and Vance, J.E. (2000) Phosphatidylserine synthase-1 and -2 are localized to mitochondria-associated membranes. *J Biol Chem* **275:** 34534-34540.

Studier, F.W., and Moffatt, B.A. (1986) Use of bacteriophage T7 RNA polymerase to direct selective high-level expression of cloned genes. *J Mol Biol* **189:** 113-130.

Studier, F.W., Rosenberg, A.H., Dunn, J.J., and Dubendorff, J.W. (1990) Use of T7 RNA polymerase to direct expression of cloned genes. *Meth Enzymol* **185:** 60-89.

Tan, T., Ozbalci, C., Brugger, B., Rapaport, D., and Dimmer, K.S. (2013) Mcp1 and Mcp2, two novel proteins involved in mitochondrial lipid homeostasis. *J Cell Sci* **126:** 3563-3574.

Tang, B.L. (2015) MIRO GTPases in Mitochondrial Transport, Homeostasis and Pathology **5:** 1.

Trotter, P.J., Pedretti, J., and Voelker, D.R. (1993) Phosphatidylserine decarboxylase from Saccharomyces cerevisiae. Isolation of mutants, cloning of the gene, and creation of a null allele. *J Biol Chem* **268:** 21416-21424.

Trotter, P.J., and Voelker, D.R. (1995) Identification of a non-mitochondrial phosphatidylserine decarboxylase activity (PSD2) in the yeast Saccharomyces cerevisiae. *J Biol Chem* **270:** 6062-6070.

van der Laan, M., Bohnert, M., Wiedemann, N., and Pfanner, N. (2012) Role of MINOS in mitochondrial membrane architecture and biogenesis. *Trends Cell Biol* **22:** 185-192.

Vance, J.E., and Steenbergen, R. (2005) Metabolism and functions of phosphatidylserine. *Prog Lipid Res* **44:** 207-234.

Vander Heiden, M.G., Chandel, N.S., Li, X.X., Schumacker, P.T., Colombini, M., and Thompson, C.B. (2000) Outer mitochondrial membrane permeability can regulate coupled respiration and cell survival. *Proc Natl Acad Sci U S A* **97:** 4666-4671.

Voelker, D.R. (1997) Phosphatidylserine decarboxylase **1348:** 236-244.

Wadhwa, R., Taira, K., and Kaul, S.C. (2002) An Hsp70 family chaperone, mortalin/mthsp70/PBP74/Grp75: what, when, and where?. *Cell Stress Chaperones* **7:** 309-316.

Waizenegger, T., Stan, T., Neupert, W., and Rapaport, D. (2003) Signal-anchor domains of proteins of the outer membrane of mitochondria: structural and functional characteristics. *J Biol Chem* **278:** 42064-42071.

Wenz, L., Opaliński, Ł., Schuler, M., Ellenrieder, L., Ieva, R., Böttinger, L.*, et al.* (2014) The presequence pathway is involved in protein sorting to the mitochondrial outer membrane. *EMBO Rep*.

Westermann, B., and Neupert, W. (2000) Mitochondria−targeted green fluorescent proteins: convenient tools for the study of organelle biogenesis in Saccharomyces cerevisiae. *Yeast* **16:** 1421-1427.

Yaffe, M.P., Jensen, R.E., and Guido, E.C. (1989) The major 45-kDa protein of the yeast mitochondrial outer membrane is not essential for cell growth or mitochondrial function. *J Biol Chem* **264:** 21091-21096.

Zerbes, R.M., Bohnert, M., Stroud, D.A., von der Malsburg, K., Kram, A., Oeljeklaus, S.*, et al.* (2012) Role of MINOS in mitochondrial membrane architecture: cristae morphology and outer membrane interactions differentially depend on mitofilin domains. *J Mol Biol* **422:** 183-191.

Zhao, X., Muller, E.G., and Rothstein, R. (1998) A suppressor of two essential checkpoint genes identifies a novel protein that negatively affects dNTP pools. *Mol Cell* **2:** 329-340.

Figure 1

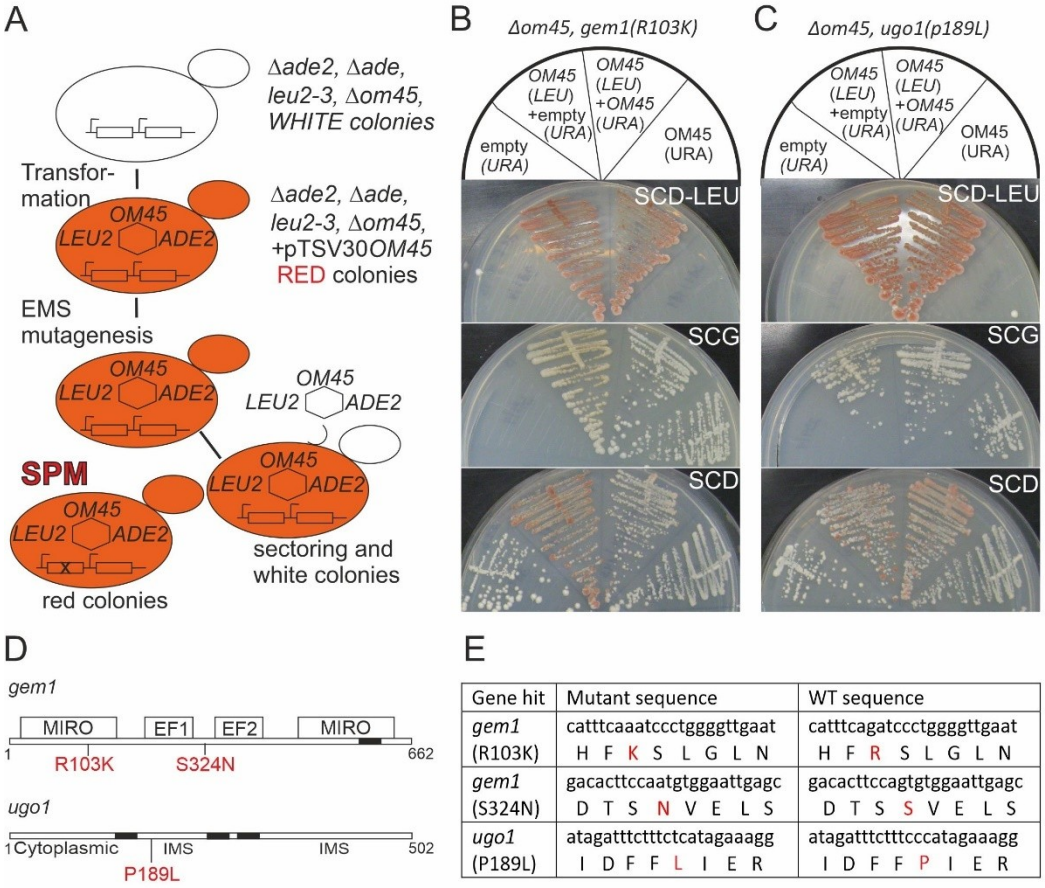

Gene hit	Mutant sequence	WT sequence
gem1 (R103K)	catttcaaatccctggggttgaat H F K S L G L N	catttcagatccctggggttgaat H F R S L G L N
gem1 (S324N)	gacacttccaatgtggaattgagc D T S N V E L S	gacacttccagtgtggaattgagc D T S S V E L S
ugo1 (P189L)	atagatttctttctcatagaaagg I D F F L I E R	atagatttctttcccatagaaagg I D F F P I E R

Figure 2

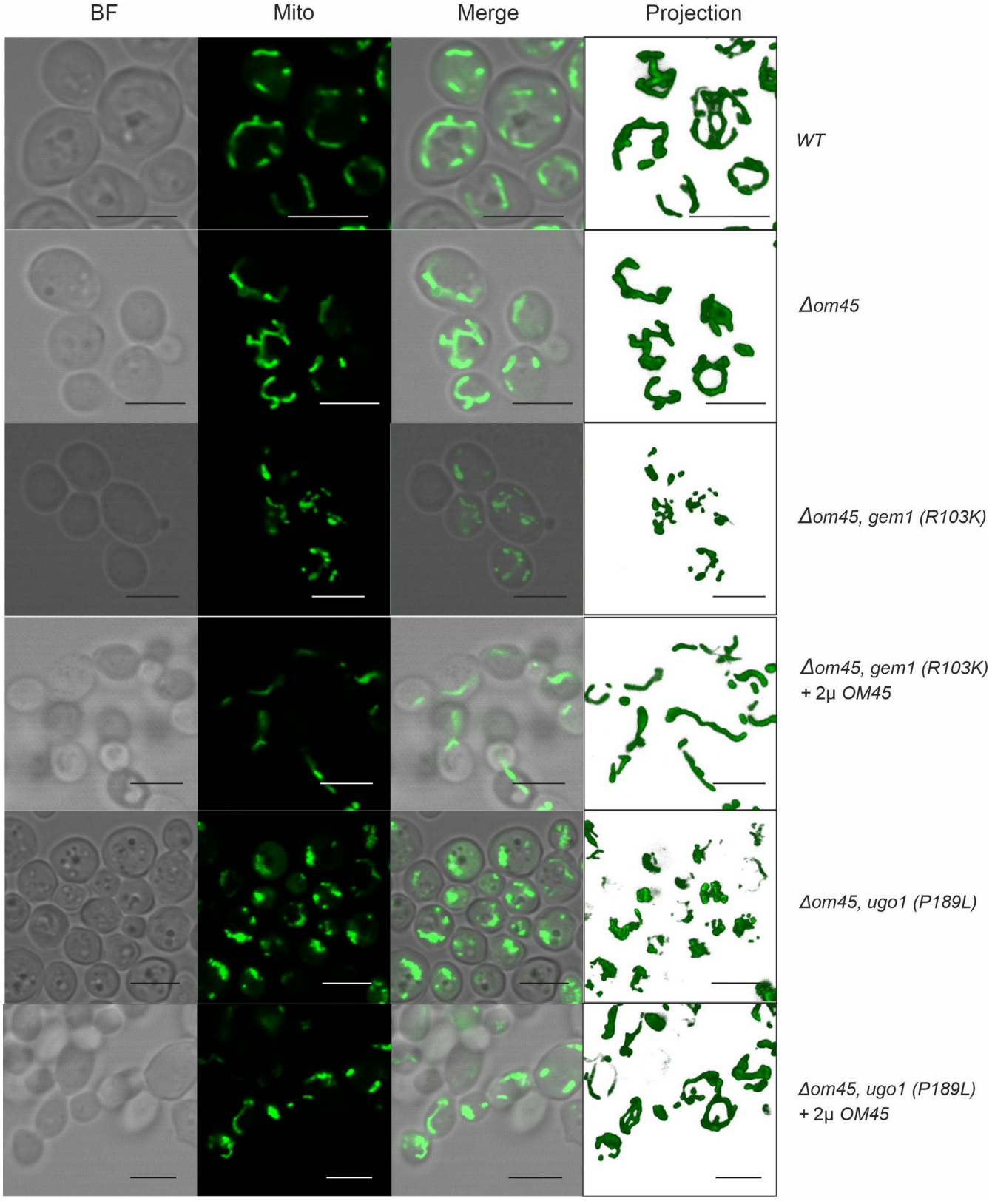
BF
Mito
Merge
Projection
WT
Δom45
Δom45, gem1 (R103K)
Δom45, gem1 (R103K) + 2μ OM45
Δom45, ugo1 (P189L)
Δom45, ugo1 (P189L) + 2μ OM45

Figure 3

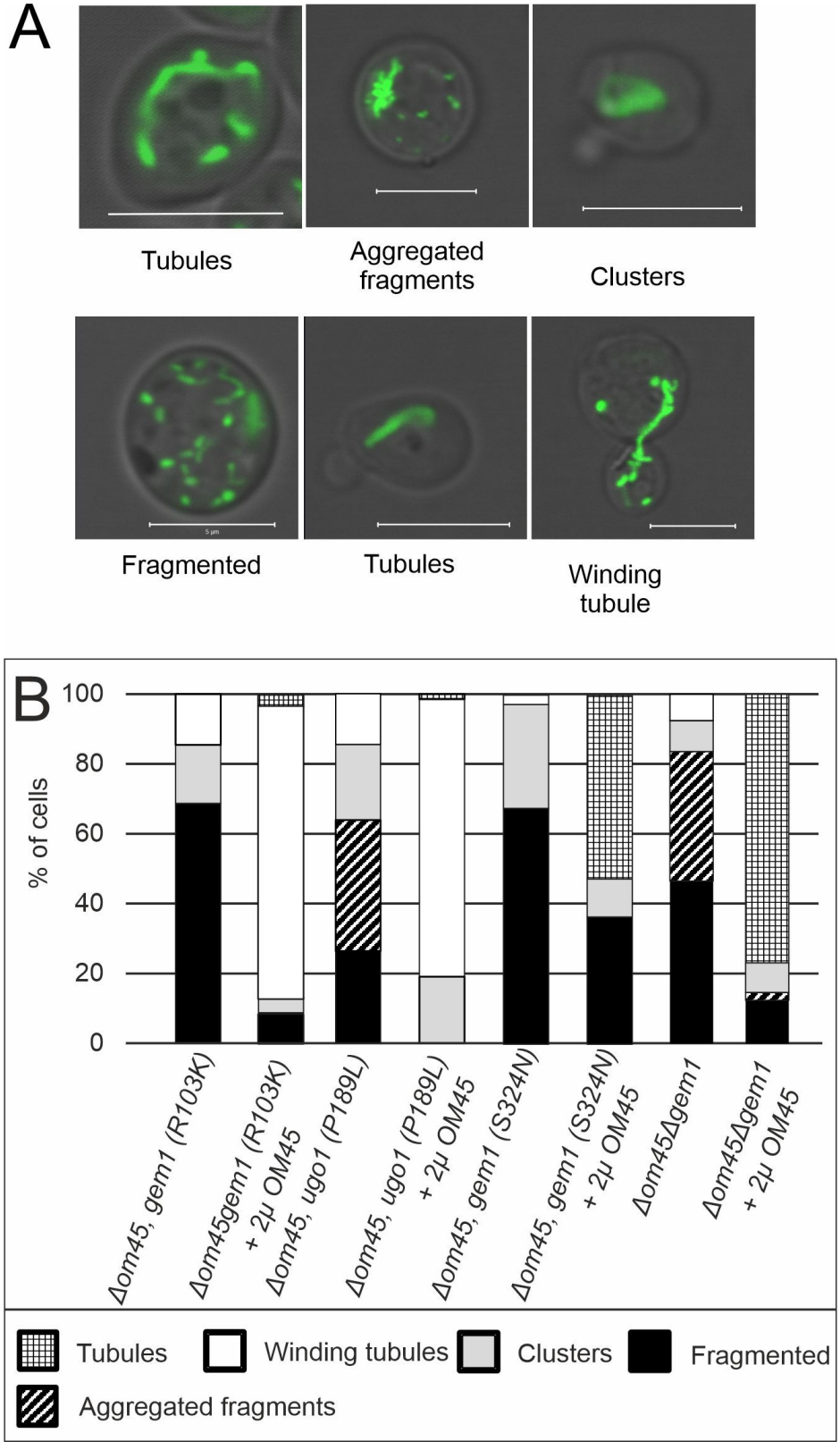
A
Tubules
Aggregated fragments
Clusters
Fragmented
Tubules
Winding tubule
B
% of cells
100
80
60
40
20
0
Δom45, gem1 (R103K)
Δom45gem1 (R103K) + 2μ OM45
Δom45, ugo1 (P189L)
Δom45, ugo1 (P189L) + 2μ OM45
Δom45, gem1 (S324N)
Δom45, gem1 (S324N) + 2μ OM45
Δom45Δgem1
Δom45Δgem1 + 2μ OM45
Tubules
Winding tubules
Clusters
Fragmented
Aggregated fragments

Figure 4

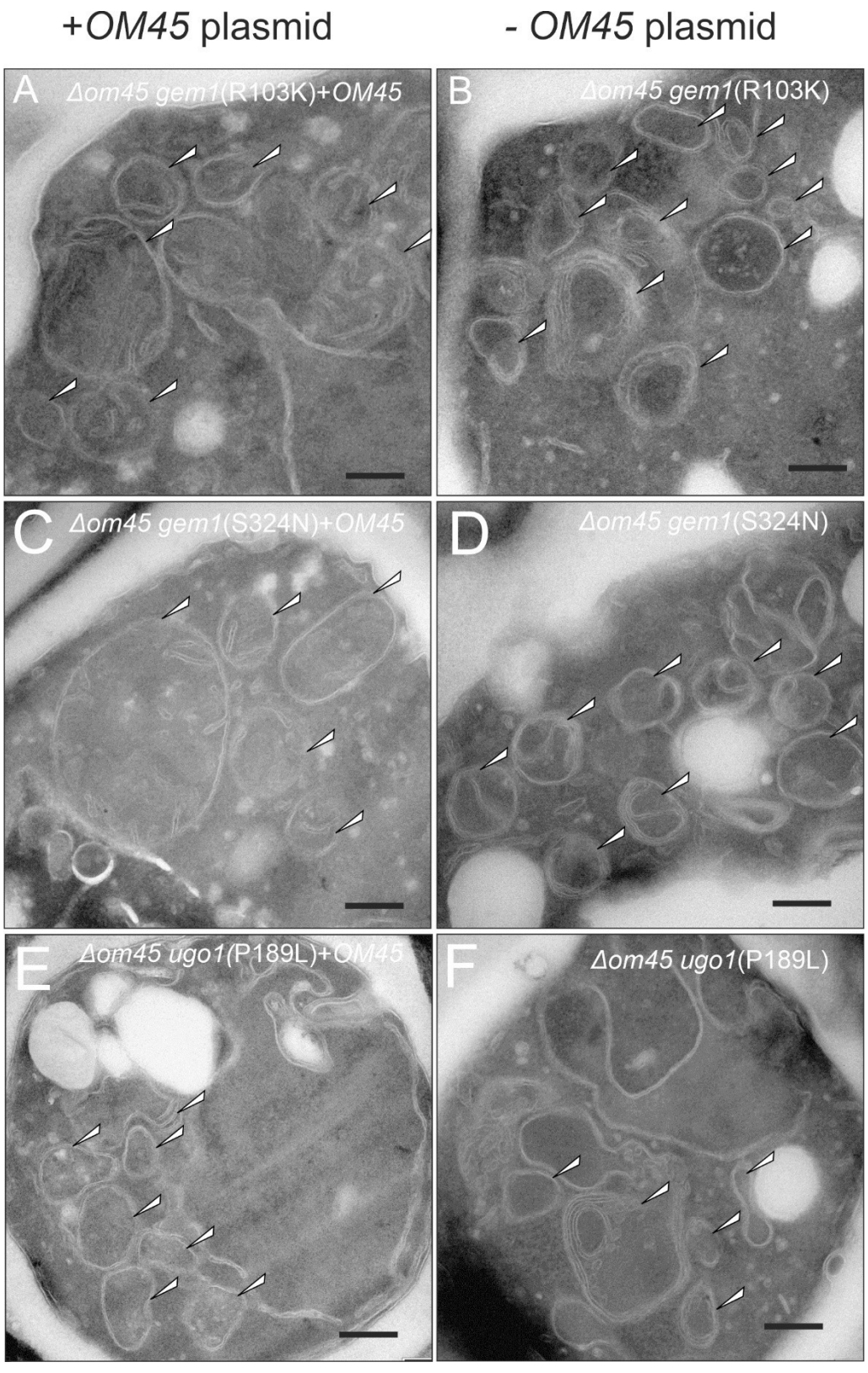
+OM45 plasmid
- OM45 plasmid
A Δom45 gem1(R103K)+OM45
B Δom45 gem1(R103K)
C Δom45 gem1(S324N)+OM45
D Δom45 gem1(S324N)
E Δom45 ugo1(P189L)+OM45
F Δom45 ugo1(P189L)

Figure 5

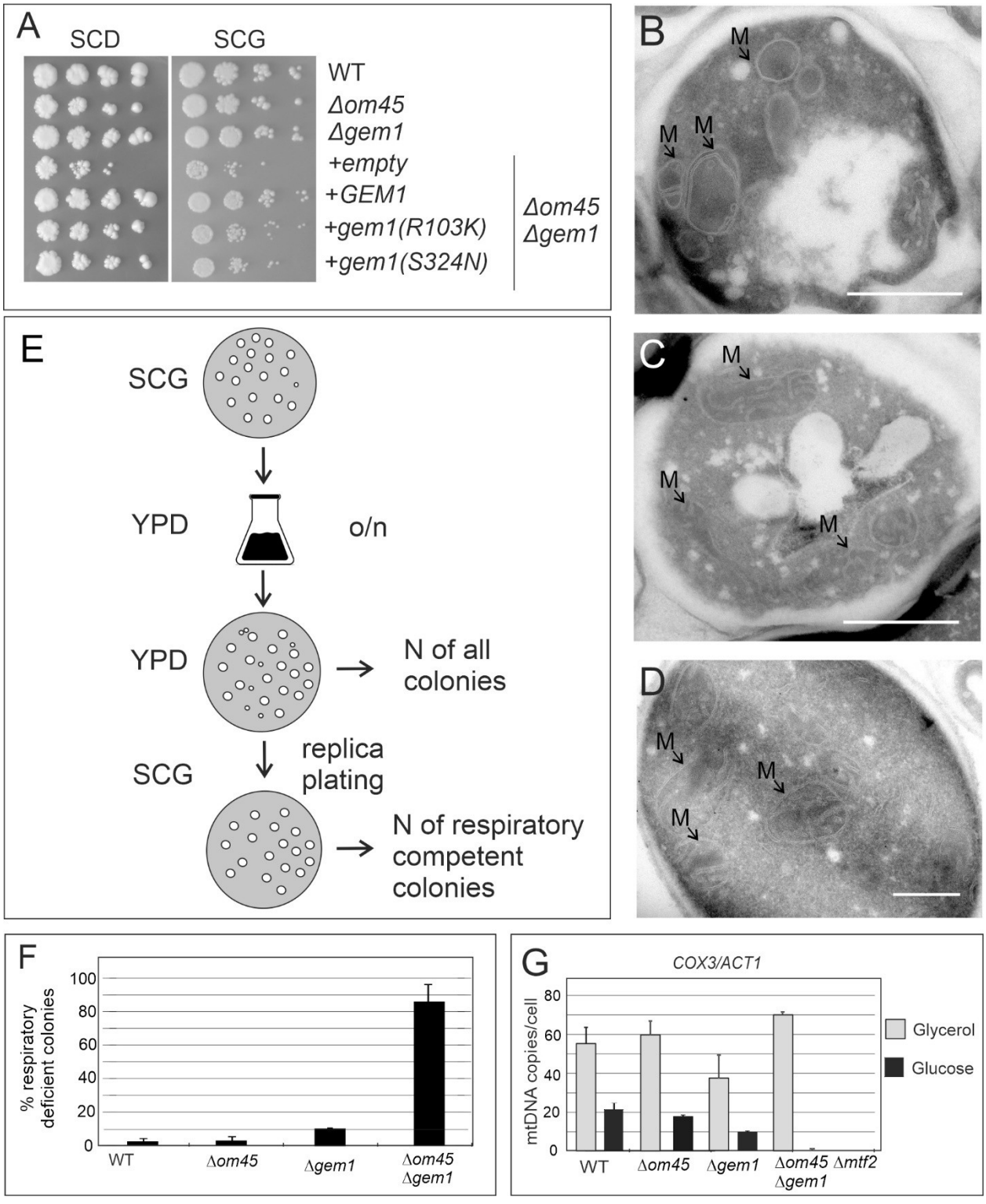
A
SCD
SCG
WT
Δom45
Δgem1
+empty
+GEM1
+gem1(R103K)
+gem1(S324N)
Δom45 Δgem1
B
C
D
M
E
SCG
YPD
o/n
YPD
N of all colonies
SCG
replica plating
N of respiratory competent colonies
F
% respiratory deficient colonies
100
80
60
40
20
0
WT
Δom45
Δgem1
Δom45 Δgem1
G
COX3/ACT1
mtDNA copies/cell
80
60
40
20
0
Glycerol
Glucose
WT
Δom45
Δgem1
Δom45 Δgem1
Δmtf2

Figure 6

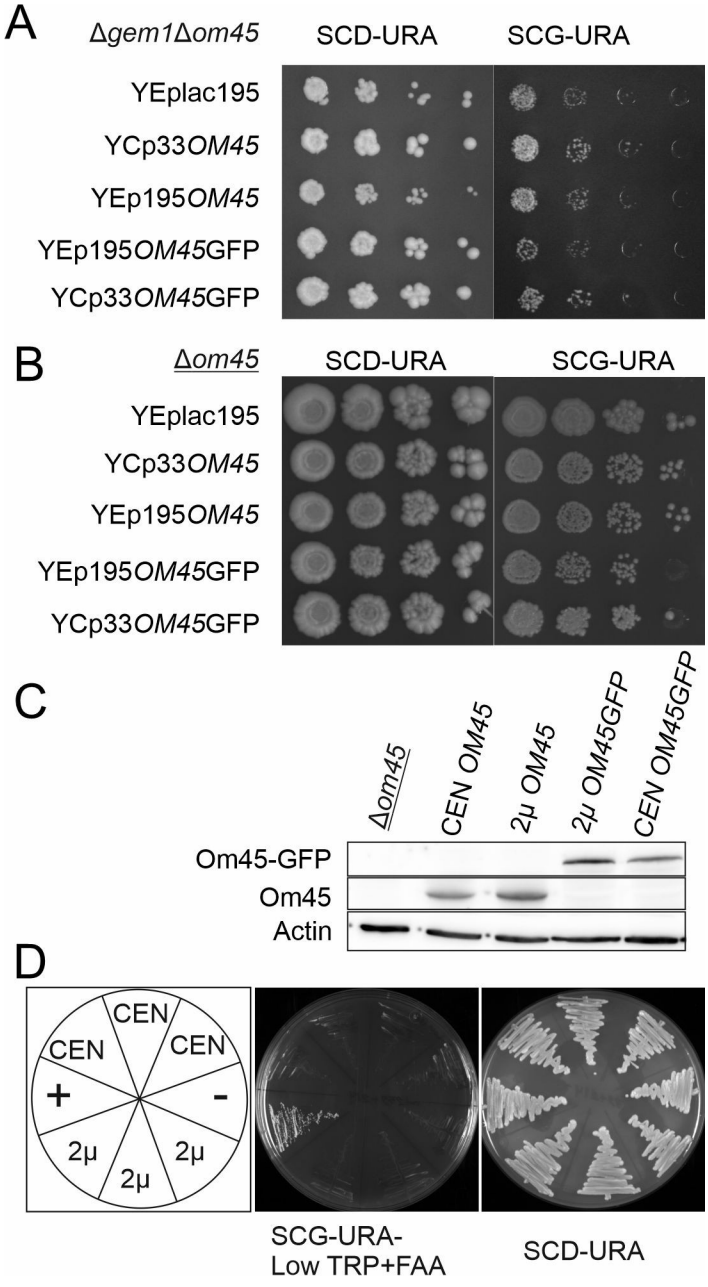
A
Δgem1Δom45
SCD-URA
SCG-URA
YEplac195
YCp33OM45
YEp195OM45
YEp195OM45GFP
YCp33OM45GFP
B
Δom45
SCD-URA
SCG-URA
YEplac195
YCp33OM45
YEp195OM45
YEp195OM45GFP
YCp33OM45GFP
C
Δom45
CEN OM45
2μ OM45
2μ OM45GFP
CEN OM45GFP
Om45-GFP
Om45
Actin
D
CEN
CEN
CEN
+
-
2μ
2μ
2μ
SCG-URA-
Low TRP+FAA
SCD-URA

Supplementary Figure 1. Growth phenotype of W1536 8B wild type and om45 deletion strain on different growth media.

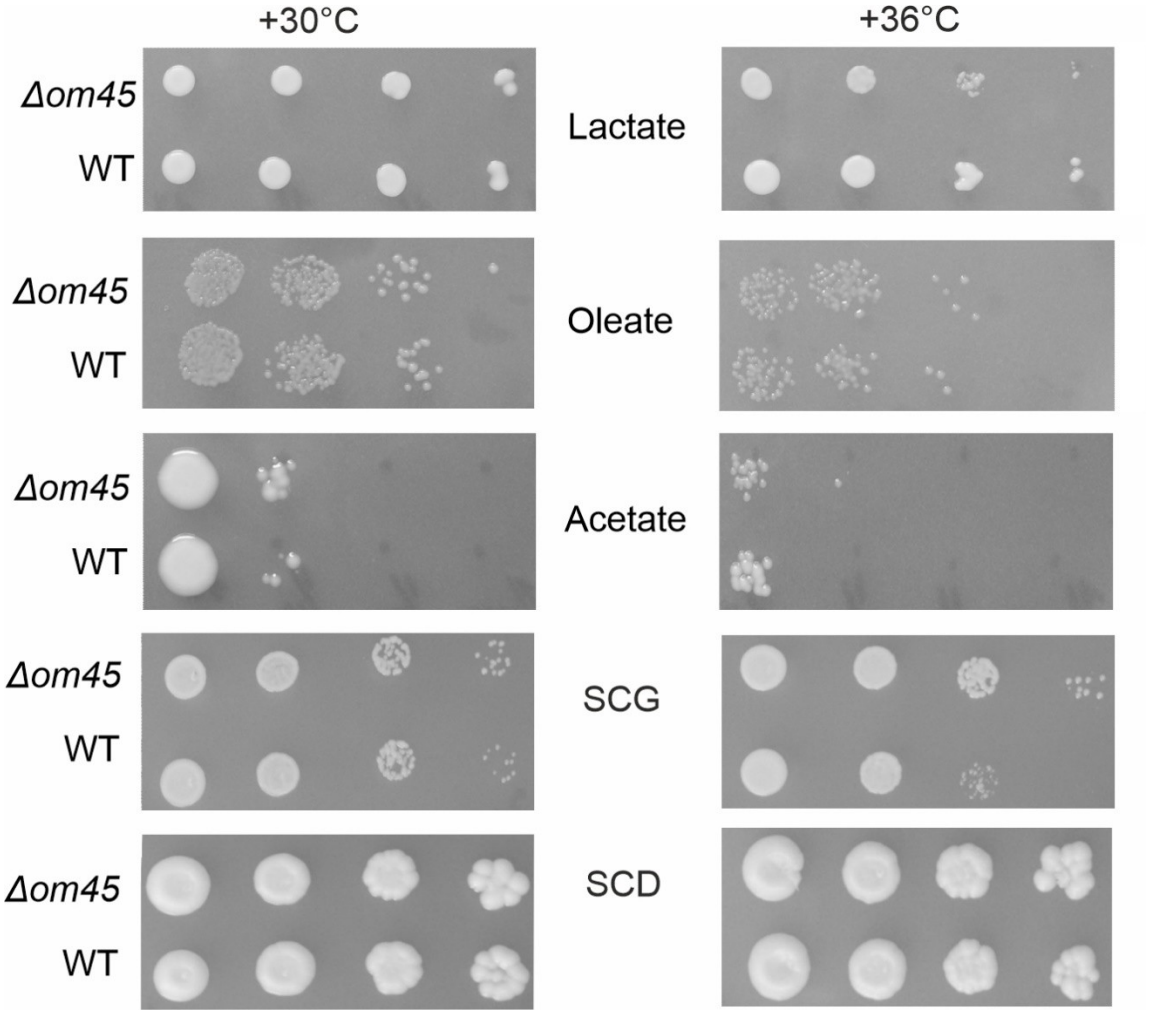

Supplementary Figure 2. Tetrad dissection of SPMs

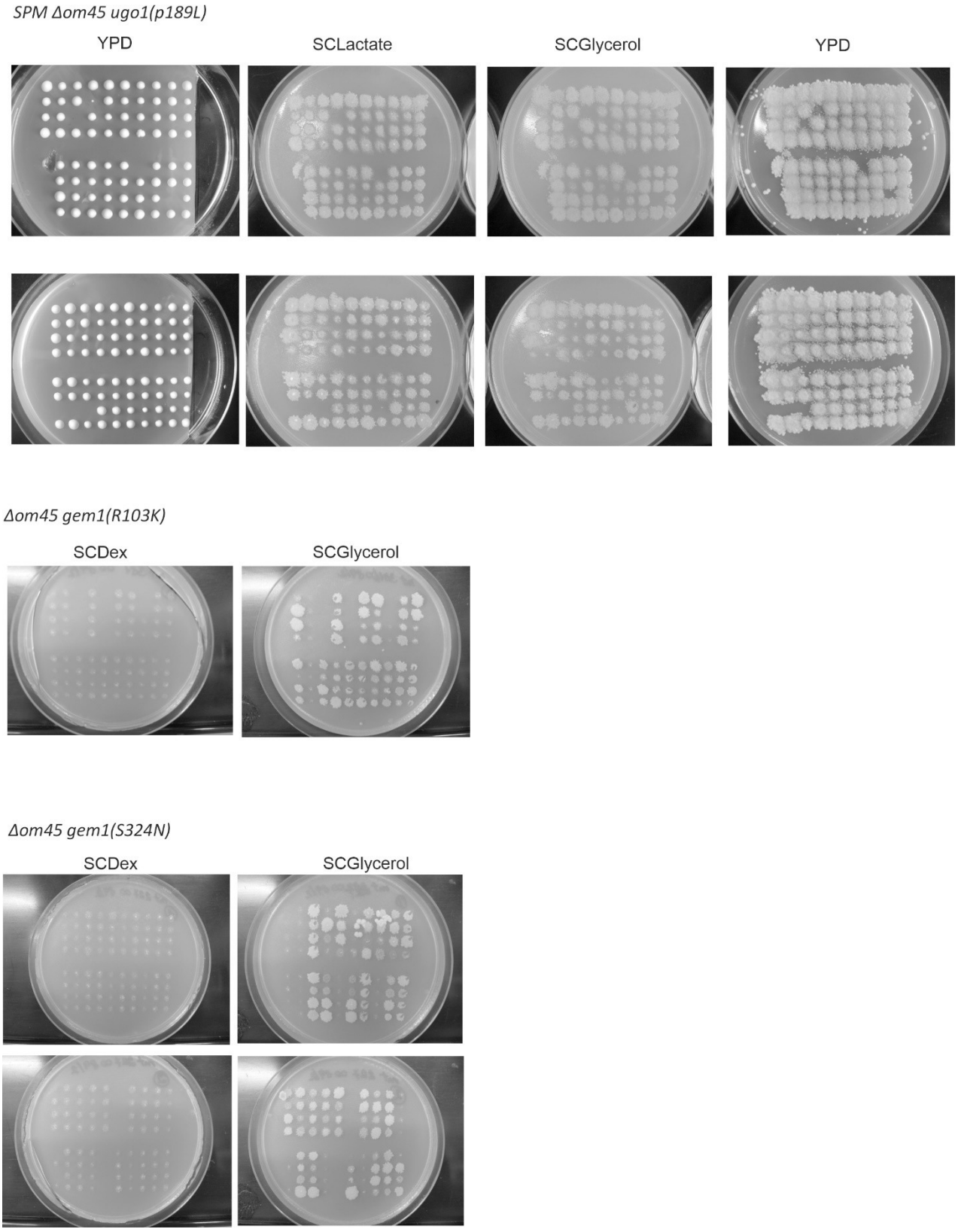

Supplementary figure 3: Growth of the reconstructed of Δ*om45/ugo1* SPM

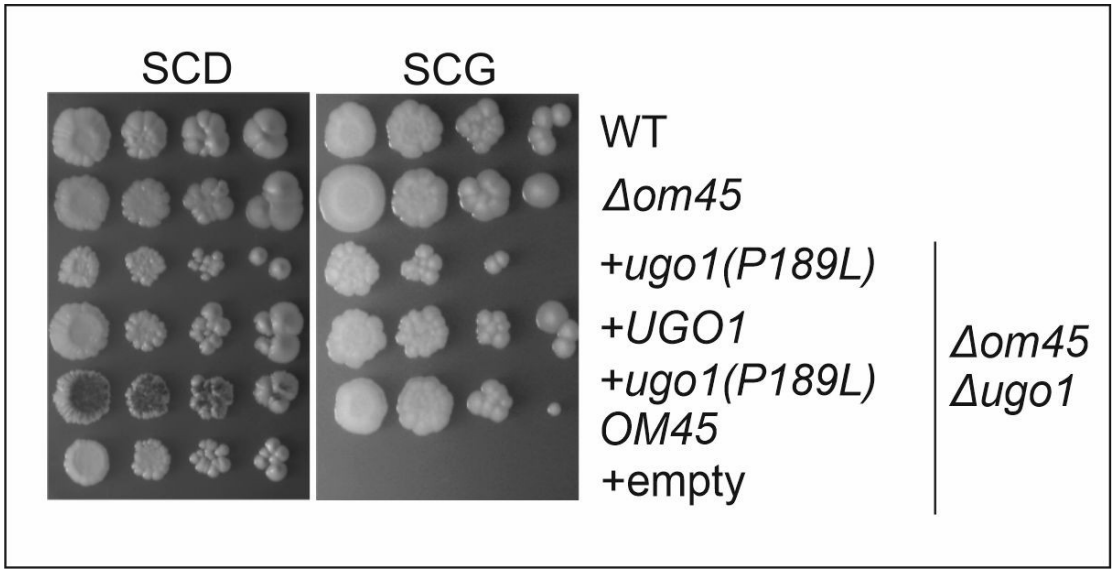

Supplementary Figure 4. Mitochondrial morphology changes and mtDNA loss in the SPMs.

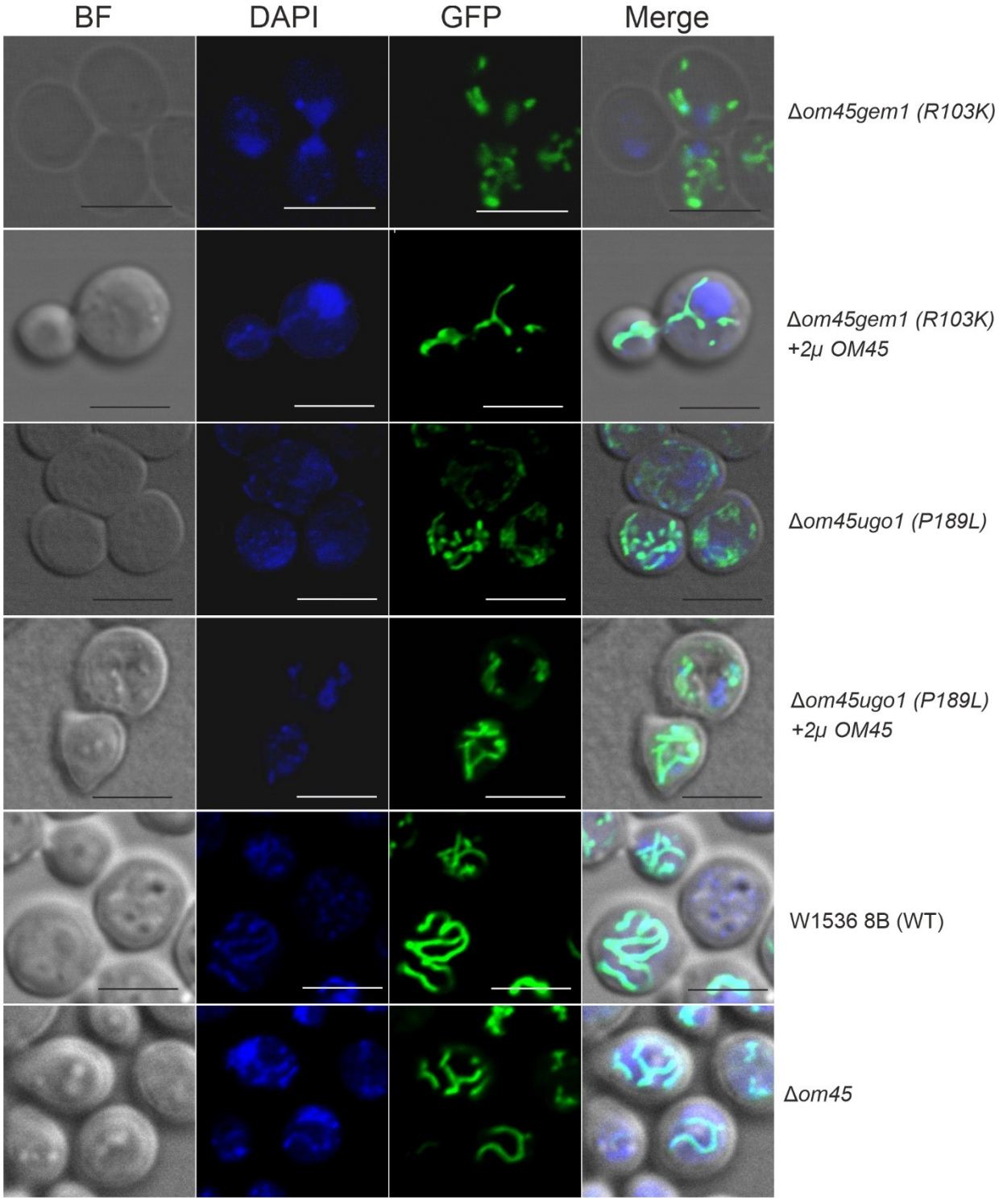

Supplementary Figure 5: Growth assay of the W1536 8B*Δom45, ugo1(P189L)* mutant transformed with multicopy suppressor plasmids

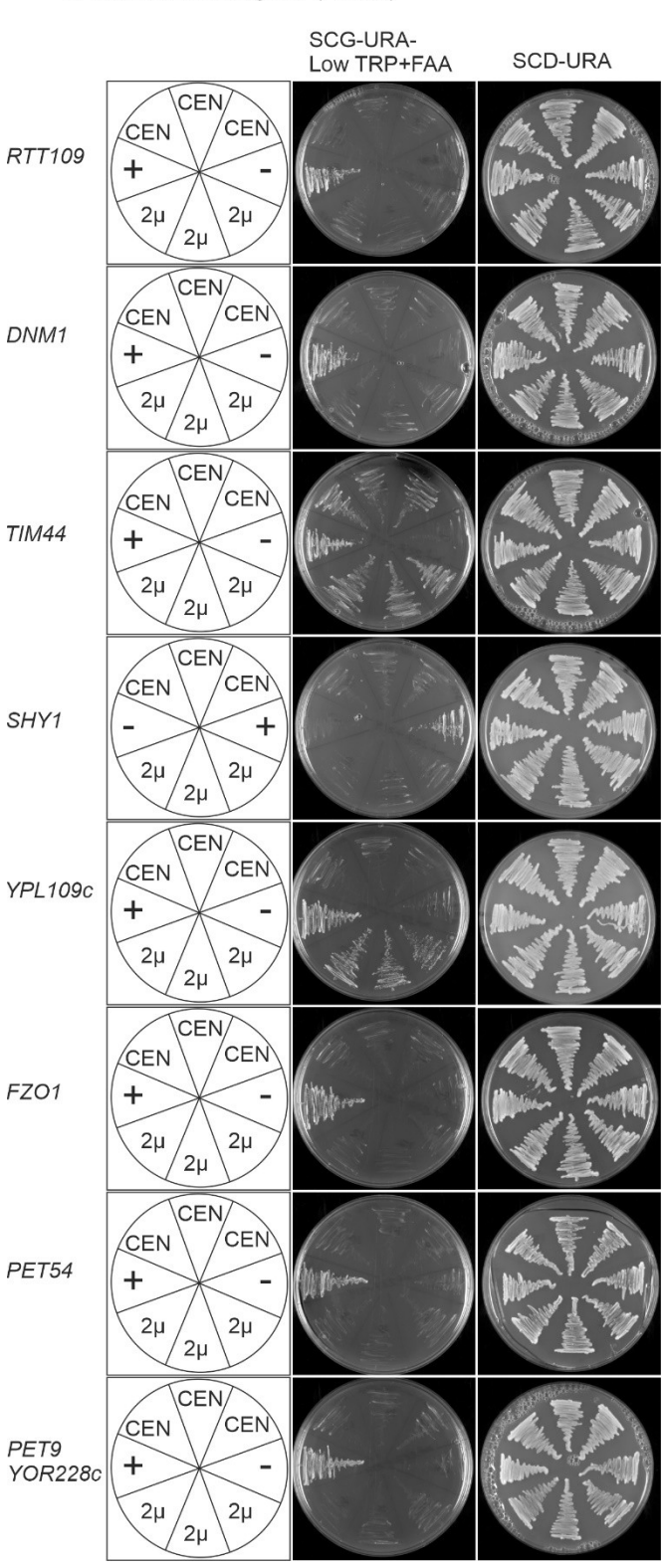

Supplementary Figure 6: Growth assay of the W1536 8BΔom45, gem1(R103K) mutant transformed with multicopy suppressor plasmids

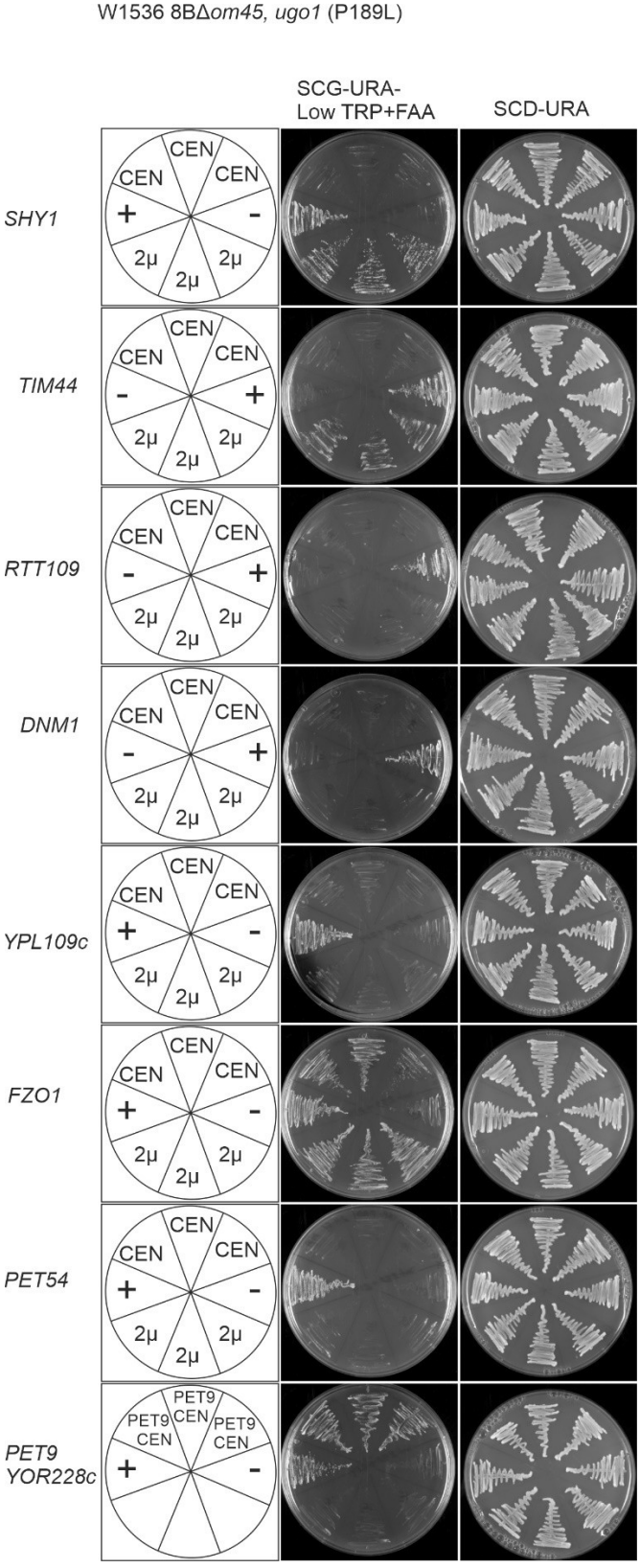

SUPPLEMENTARY TABLE 1

Library plasmids rescuing the respiratory deficient phenotype of the SPMs.

	Chromosome			Genes on the plasmid	Growth rescue		
	Number	from	to		*Δom45, gem1* (S324N)	*Δom45, gem1* (R103K)	*Δom45, ugo1* (P189L)
Isolated from synthetic petite mutant Δo*m45*, *gem1* (S324N)							
L	X	204547	209917	*MDV1,CCT7*	3/3 weak		
L	III	175407 175411	178862 178866	*RPS14A,SNR65SNR189*			
L	X	39879	41655	*NUC1*	1/3 weak	1/3 weak	
H	VII	937532	942532	***PET54***	3/3 weak	0/3	
	VII	937396	940318	***PET54***	3/3 weak	0/3	
L	IV	1320450	1325454	*RPN9,YDR426C,BNA7,TIF35*	3/3 weak	3/4 weak	
L	not sequenced				3/3 weak	3/3 weak	
L	I	50217 52050	55793 55793	*AIM2,**GEM1***	3/3	3/3	3/3
Isolated from synthetic petite mutant Δom45, *ugo1* (P189L)							
	II	575000	595000	***FZO1***	0/3	0/3	3/3
	IV	1399442	1407105	***UGO1***	0/3	0/3	3/3
L	II	162308	167700	***PET9***	3/3	3/3	3/3
	IX	79000	99000	*OM45*			
	VII	715554	719176	*YGR111,* ***SHY1***	3/3	3/3	3/3
	XIV	386997	392422	*EXBP6,SPC98*			
L	IX	309455	313798	***TIM44***, *RPB3*	3/3 weak	0/3	no
	IX	82000	102000	*OM45*			
L		145655	150076	***RTT109***, *DNM1*	NO	3/3 weak	(0/6)
Isolated from synthetic petite mutant Δom45, *gem1* (R103K)							
L	VII	932885	940245	***PET54*** others			
L	VII	937760	946051	***PET54*** others	3/3	3/3 weak	
L	IX	93574	97460	*OM45*	3/3	3/3	
L	not sequenced				3/3 weak	4/4 weak	
L	XV	102337	102577	truncation of *PAP2*	3/3 weak	3/3 weak	
L					3/3 weak	0/3	
L	not sequenced				3/3 weak	3/3 weak	
H	V	116587	117048	URA3	3/3 weak		
H	not sequenced				3/3 weak	3/3 weak	
H	XV	766540	767312	*WTM2,* ***YOR228C***	3/3	2/3	
H	not sequenced				3/3 weak	1/3 weak	

	Chromosome			Genes on the plasmid	Growth rescue		
	Number	from	to		*Δom45, gem1* (S324N)	*Δom45, gem1* (R103K)	*Δom45, ugo1* (P189L)
H	XVI	830340	834690	*YPR150W, SUE1,URN 1,YPR153W (ECM10)* ***SSC3***	3/3 weak	0/3	
L	V	91739	97260	*GEM1*	3/3 weak	7/7 weak	
L	I	52050	56140	***GEM1***	3/3	3/3	
H	IX	94170	94363	*OM45*	2/2	3/3	
L	VI	52051	56163	***GEM1***	3/3	3/3	
H	XVI	341371	341810	truncation of *GDE1*			
L	XVI	341370	348068	***YPL109C***, *GDE1*	3/3	3/3	
L	V	116676	117010	*URA3*	3/3 weak	0/3	
L	IX	307795	313463	***TIM44***	3/3	3/3	3/3
L	XI	384109	390299	*YKL027w, TFA1*	0/3	0/3	
L	not sequenced				3/3 weak	3/3 weak	

For origin of the plasmid: L- Lacroute library, H- HeAl library. The plasmids are presented in the order of mutants found complemented, although eventually suppression was tested in all three mutants. Chromosome number as well as location are indicated with numbers. Since multiple ORFs were present on most of the library plasmids, the underlined genes were confirmed as rescuing component after subcloning to a separate multiple and single copy vectors. Rescue x/y numbers indicate number of growing clones (x) out of tested (y). "weak" indicate very weak growth of the rescued colonies. Empty fields: Not tested.

1274
1275
1276
1277
1278
1279

Supplementary Figure 7: Whole cell and mitochondrial phospholipidome analysis of W1536 8B Δ*psd2*, W1536 8B Δ*psd2*Δ*om45*, W1536 8B Δ*psd2*Δ*gem1*, W1536 8B Δ*psd2*Δ*om45*Δ*gem1* and W1536 8B Δ*psd2*Δ*psd1* strains.